THE QUANTUM MECHANICS OF THE SCALAR FIELD IN THE NEW INFLATIONARY UNIVERSE

Alan H. Guth*

Center for Theoretical Physics
Laboratory for Nuclear Science and Department of Physics
Massachusetts Institute of Technology
Cambridge, Massachusetts 02139

and

Harvard-Smithsonian Center for Astrophysics
60 Garden Street
Cambridge, Massachusetts 02138

and

So-Young Pi†

Department of Physics
Boston University
Boston, Massachusetts 02215

*This work was supported in part through funds provided by the U.S. Department of Energy (DOE) under contract DE-AC02-76ER03069, in part by the National Aeronautics and Space Administration (NASA) under grant NAGW-553, and in part by an Alfred P. Sloan Fellowship.

†This work was supported in part through funds provided by the Department of Energy under the Outstanding Junior Investigator Program.

CTP# 1246

March, 1985

ABSTRACT

An attempt is made to clarify the quantum theory of the "slow-rollover" phase transition which characterizes the new inflationary universe model. We discuss the theory of the upside-down harmonic oscillator as a toy model, with particular emphasis on the fact that the system can be described at late times by a classical probability distribution. An approximate but exactly soluble model for the scalar field is then constructed, based on three principal assumptions: 1) exact de Sitter expansion for all time; 2) a quadratic potential function which changes from stable to unstable as a function of time; and 3) an initial state which is thermal in the asymptotic past. It is proposed that this model would be the proper starting point for a perturbative calculation in more realistic models. The scalar field can also be described at late times by a classical probability distribution, and numerical calculations are carried out to illustrate how this distribution depends on the parameters of the model. For a suitable choice of these parameters, a sufficient period of inflation can be easily obtained. Density fluctuations can be calculated exactly in this model, and the results agree very well with those previously obtained using approximate methods.

I. Introduction

The new inflationary universe model[1,2,3,4] seems to provide a highly attractive picture for the early evolution of our universe. By hypothesizing a significant modification of the standard hot big bang model at a time scale of about 10^{-35} sec, the model offers a possible explanation for a number of the most salient properties of the observed universe. It explains the large scale homogeneity and isotropy of the universe, and it also explains why the quantity Ω (the ratio of the actual mass density to the critical mass density) lies so close to the unstable value of unity. In the context of grand unified theories, the inflationary model also provides a natural mechanism for avoiding the tremendous overproduction of magnetic monopoles which occurs when standard cosmology is extrapolated back to the grand unified theory epoch. In addition, the model provides a framework for predicting the spectrum of primordial density fluctuations[5] responsible for the origin of galactic structure. And finally, if the model is correct, it would mean that we understand the production mechanism for essentially all the matter, energy, and entropy in the observed universe.

The key feature of the new inflationary model is a phase transition of a special type, often called a "slow-rollover" transition. This type of transition was introduced by Linde,[2] and independently by Albrecht and Steinhardt,[3] to overcome some crucial problems which had been discovered[6] in the original version[1] of the model. The name "slow rollover" arises because the transition involves a scalar field[7] which evolves slowly down a gentle hill in its potential energy diagram. The purpose of this paper[8] is to present a new and more detailed treatment of the quantum behavior of this scalar field, particularly during the earliest stages of the slow rollover. These quantum effects are very important for several reasons. First, they control the length of time for which the scalar field remains near the top of the hill in the potential energy diagram, and hence they determine the duration of the inflationary era. In addition, quantum fluctuations provide the source of mass density fluctuations which are the likely seeds for the origin of galactic structure. Our research in this area is continuing, but so far we have constructed and solved an approximate model which will be described in this paper.

To discuss the motivation for this new treatment, we begin by summarizing what

can be regarded as the standard picture for the behavior of the scalar field. The generic behavior of the finite temperature effective potential is shown qualitatively in Figure 1. The curves have been shifted vertically so that they all coincide at $\phi = 0$. At zero temperature the potential is extremely flat near $\phi = 0$, and $V(\phi = 0) \equiv \rho_0$; $V(\phi)$ has a minimum at $\phi = \phi_c$. At extremely high temperatures ($T \gg$ critical temperature T_c) the effective potential has a unique minimum at $\phi = 0$. As the universe cools the scalar field ϕ gets caught at $\phi \approx 0$, in a state which is called a false vacuum.[9] The equation of state for this false vacuum causes the universe to rapidly evolve into a de Sitter space,[10] which can be described by the metric

$$ds^2 \equiv g_{\mu\nu} dx^\mu dx^\nu = -dt^2 + e^{2\chi t} d\vec{x}^2, \tag{1.1}$$

where the expansion rate χ is related to the energy density ρ_0 of the false vacuum. The scalar field hovers for a while at $\phi \approx 0$, and then eventually begins to roll down the hill of the potential energy diagram, obeying the classical de Sitter space equation of motion

$$\ddot{\phi} + 3\chi\dot{\phi} - e^{-2\chi t}\vec{\nabla}^2\phi = -\frac{\partial V}{\partial \phi}, \tag{1.2}$$

where

$$\vec{\nabla}^2 \equiv \sum_{i=1}^{3} \frac{\partial^2}{\partial (x^i)^2}. \tag{1.3}$$

The inflationary era occurs during this slow rollover. The homogeneous solution to the classical equations of motion will be called $\phi = \phi_0(t)$.

The scalar field is of course not entirely classical, so quantum fluctuations about the classical solution must be taken into account.[5] These quantum fluctuations produce inhomogeneities in the scalar field

$$\phi(\vec{x}, t) = \phi_0(t) + \delta\phi(\vec{x}, t), \tag{1.4}$$

which in turn give rise eventually to inhomogeneities in the mass density of the universe. Assuming that $|\delta\phi| \ll \phi_0$, the perturbation can be treated as a free quantum field obeying

the linearized equation

$$\ddot{\delta\phi} + 3\chi\,\dot{\delta\phi} - e^{-2\chi t}\vec{\nabla}^2\,\delta\phi = -\frac{\partial^2 V}{\partial\phi^2}(\phi_0)\,\delta\phi. \qquad (1.5)$$

Using these ideas, it is then possible to calculate the resulting spectrum of mass density perturbations. (For more details, see Section VII.)

This standard picture relies on a number of assumptions, and various questions have been raised about its validity:

1. Is the picture of a classical slow rollover valid? It has been pointed out by Mazenko, Unruh, and Wald[11] that at high temperatures, when one says that $\phi \approx 0$, one really means that the spatial or time average of ϕ is about equal to zero— the field itself is undergoing large fluctuations. As the system cools, they argue, it is possible that these fluctuations, which extend initially out to $\phi = \pm\phi_c$ or more, will cause the scalar field to settle quickly into small regions with $\phi \approx \pm\phi_c$ in each of these regions. When one looks at the spatial average one might see what appears to be a rolling motion, but the actual local dynamics could be quite different. In particular, these authors claim that the picture of a classical slow rollover is invalid for Coleman-Weinberg models[12,2,3] with $g^2 \approx 1$, and also for all models in which the scalar field which drives the inflation interacts only with itself. We find, however, that self-interacting scalar field models appear perfectly acceptable provided that the coupling constant is sufficiently small. Presumably a similar statement could be made for the Coleman-Weinberg case, although we do not study the case in this paper. On the other hand, our results agree with Mazenko, Unruh, and Wald for cases with couplings of order unity.

2. What is the physical significance of the classical function $\phi_0(t)$? Hawking and Moss[13] point out that the system begins in a thermal ensemble which possesses an exact symmetry, $\phi \to -\phi$. The dynamics is also consistent with this symmetry, and it therefore follows that $<\phi(\vec{x},t)>$ remains zero for all time the field presumably does roll down the hill, but since it is equally likely to roll in any direction, the expectation value remains zero. Hawking and Moss developed

an alternative method of calculation in which only the operator $\phi^2(\vec{x},t)$ appears. Using this method, they calculated[13] a value for the fluctuation amplitude which was in significant disagreement with calculations done using the standard picture.[5] These authors have since retracted their calculation,[14] but the question which they raise still requires an answer. In our method of calculation, $\phi_0(t)$ will be given a very explicit meaning.

3. The standard picture described above gives no prediction for how long the scalar field will hover about $\phi = 0$ before it begins rolling down the hill of the effective potential. This question is of course crucial, since it determines whether or not sufficient inflation is obtained. The question has been studied by Linde[15] and by Vilenkin and Ford[16], who calculated the behavior of $<\phi^2(t)>$. This operator is infinite and requires a subtraction, and it was never completely clear to us how this expectation value is related to the behavior of ϕ itself. Our methods will address this question in what we feel is a more precise way, but we should say at the beginning that our results are in qualitative agreement with the results of these previous authors.

4. It is well known[17] that the effective potential shown in Figure 1 is actually ill-defined. In particular, the behavior shown for the zero temperature potential at $\phi < \phi_c$ violates rigorous convexity theorems. The shape of the true effective potential depends on choices made in its definition. One choice leads to a Maxwell construction, $V(\phi) = 0$ for $|\phi| < \phi_c$. Another choice, based on analytic continuation in the parameters of the theory, leads to an effective potential which is complex when $|\phi| < \phi_c$. In the light of these statements, it is not clear that the standard picture is reliable. The problem is essentially that the standard picture attempts to describe a time-dependent situation using the effective potential, which is a quantity defined to describe static, equilibrium situations. Our method will avoid this question, since it will involve a dynamical calculation which makes no use of the effective potential.

The goal of the present work is to provide answers to these questions. In order to

do this we have constructed an approximate model for the behavior of the scalar field in the new inflationary universe. The virtue of this approximate model is that it is a free field theory, and therefore exactly soluble. It is of course unrealistic, but we claim that the model qualitatively describes the correct physics. Furthermore, we believe that it will serve as a valid zero order approximation to a more complicated calculation in which interactions are taken into account perturbatively.

The organization of the paper is as follows. In Section II we describe the behavior of an upside-down harmonic oscillator, which we use as a toy problem which exemplifies the quantum mechanical behavior of an unstable system. In particular, we explain why the behavior of such a system at late times can be treated classically, although it is not described by a single classical trajectory— rather, it must be described by a classical probability distribution. Section III contains the core of this paper. Here we define the approximate model of the phase transition, attempting to explain clearly the assumptions on which it rests. This section also includes the mathematical solution of the model. In the following section we demonstrate that the analogy with the upside-down harmonic oscillator holds true, in that the behavior does become classical at late times. In Section V we introduce a "smeared" scalar field operator, defined by averaging the value of the true scalar field operator over a small region of space. This averaging is necessary in order to obtain an operator which in principle could be measured — a quantum field at a point is rendered unmeasurable by infinite fluctuations. Numerical results which describe the smeared scalar field are presented in Section VI. The calculation of mass density fluctuations is described in Section VII, and a summary of the conclusions is presented in Section VIII.

As this work was nearing completion, we learned that similar work was being carried out by R. Brandenberger,[18] J. M. Bardeen,[19] W. Bardeen and C. Hill.[20] In addition, A. Albrecht and R. Brandenberger[21] have written a paper which is somewhat complimentary to this one, showing that the free field approximation holds for a sufficiently long time if the couplings are small enough. Other closely related recent papers include those of G. Semenoff and N. Weiss,[22] M. Evans and J.G. McCarthy,[23] T. Banks, W. Fischler, and L.

Susskind,[24] and W. Fischler, B. Ratra, and L. Susskind.[25]

II. Quantum Mechanics of an Upside-Down Harmonic Oscillator

In this section we examine a problem in one dimensional quantum mechanics which has many similarities to the quantum field theory problem which we will discuss later. We consider a particle moving in the potential[26]

$$V(x) = -\frac{1}{2}kx^2, \qquad k > 0. \tag{2.1}$$

At $t = 0$ the particle is described by a wave function which is centered and peaked at $x = 0$. For simplicity, we choose this wave function to be a Gaussian.

The evolution is then governed by the Schrödinger equation

$$i\hbar\frac{\partial\psi}{\partial t} = -\frac{\hbar^2}{2m}\frac{\partial^2\psi}{\partial x^2} - \frac{1}{2}kx^2\psi. \tag{2.2}$$

This equation is satisfied by a wave function of the form

$$\psi(x,t) = A(t)\exp\{-B(t)x^2\}, \tag{2.3}$$

provided that

$$i\hbar\dot{A} = \hbar^2 AB/m \tag{2.4a}$$

and

$$i\hbar\dot{B} = \frac{1}{2}k + 2\hbar^2B^2/m, \tag{2.4b}$$

where a dot above a symbol denotes differentiation with respect to t. In solving these equations it is useful to introduce the parameters

$$\begin{aligned} a^2 &\equiv \hbar/\sqrt{mk}, \\ \omega^2 &\equiv k/m. \end{aligned} \tag{2.5}$$

The parameter a describes a natural quantum-mechanical length scale, analogous to the Bohr radius of the hydrogen atom. We will see that the system will appear classical when

it is probed at length scales large compared to a. In terms of these parameters, one finds

$$\begin{aligned} B &= \frac{1}{2a^2}\tan(\phi - i\omega t) \\ &= \frac{1}{2a^2}\frac{\sin 2\phi - i\sinh 2\omega t}{\cos 2\phi + \cosh 2\omega t}, \end{aligned} \tag{2.6}$$

where ϕ is a real constant of integration which is related to the width of the wave packet at $t = 0$. The differential equation is satisfied for complex values of ϕ, but we choose to absorb the imaginary part of ϕ into a redefinition of the origin of t. The wave packet is then at its minimum width when $t = 0$. For a properly normalized wave function one finds

$$A = (2\pi)^{-1/4}[b\cos(\phi - i\omega t)]^{-1/2}, \tag{2.7}$$

where

$$b = a(\sin 2\phi)^{-1/2}. \tag{2.8}$$

We are particularly interested in the behavior of $\psi(x,t)$ for large t, which is given by

$$\psi(x,t) \xrightarrow[t\to\infty]{} (2/\pi)^{1/4} b^{-1/2} e^{-\frac{1}{2}(\omega t + i\phi)} \exp\left\{-e^{-2\omega t}\frac{x^2}{b^2} + \frac{ix^2}{2a^2}\right\}. \tag{2.9}$$

The probability distribution for x is then Gaussian, with

$$< x^2 > \to \frac{1}{4} b^2 e^{2\omega t}. \tag{2.10}$$

Note that the ϕ-dependence of $< x^2 >$ is easily understood. As ϕ is varied, b^2 is minimized when $\phi = \pi/4$, with $b = a$. For $\phi < \pi/4$, the initial probability distribution for x is broad, and it therefore spreads quickly. For $\phi > \pi/4$, the initial wave function is narrowly peaked in x, and hence the spread at momentum is large; this spread of momentum results in a rapid spreading of the x-distribution.

Our main point in introducing this model is to show that the quantum mechanical wave function at large times is accurately described by classical physics. Let us first consider the commutator of the operators x and p, where $p = -i\hbar\frac{\partial}{\partial x}$. Note that[27]

$$\begin{aligned} p\psi &= \frac{\hbar x}{a^2}\psi + O(e^{-2\omega t}) \\ &= \sqrt{mk}\, x\psi + O(e^{-2\omega t}), \end{aligned} \tag{2.11}$$

where $\sqrt{mk}\, x$ is in fact the momentum which would be attained by a classical particle which rolled from rest at the peak of the potential to the point x. Let us now examine the noncommutivity of x and p:

$$xp\psi = \sqrt{mk}\, x^2\psi + O(e^{-2\omega t}) \tag{2.12a}$$

$$px\psi = \sqrt{mk}\, x^2\psi - i\hbar\psi + O(e^{-2\omega t}). \tag{2.12b}$$

The commutator contribution $-i\hbar\psi$ will be insignificant compared to the other term if $\hbar \ll \sqrt{mk}\, x^2$, or equivalently if $a^2 \ll x^2$. Thus at large times, in the region $x^2 \gg a^2$, the commutator $[x,p]$ becomes negligible and thereby poses no barrier to a classical description of the system. The general rule is that whenever the distance over which the phase of the wave function changes by 2π (i.e., the de Broglie wavelength) is much shorter than any other relevant length, then classical physics applies. Alternatively, one can say that classical physics applies whenever it is possible to ignore uncertainties Δx and Δp satisfying $\Delta x\, \Delta p \approx \hbar$.

Note however that the wave function is definitely not sharply peaked about one particular classical trajectory. Thus, the large t behavior of the system must be described not by a classical trajectory, but instead by a classical probability distribution:

$$\begin{aligned} f(x,p,t) &= |\psi(x,t)|^2 \delta(p - \sqrt{mk}\, x) \\ &= (2/\pi)^{\frac{1}{2}} b^{-1} e^{-\omega t} \exp\left\{-2e^{-2\omega t}x^2/b^2\right\}\delta(p - \sqrt{mk}\, x). \end{aligned} \tag{2.13}$$

To see that $f(x,p,t)$ provides an accurate classical description of the system at late times, one must verify the following two statements:

a) $f(x,p,t)$ describes classical physics — that is, it obeys the classical equations of motion:

$$\frac{\partial f}{\partial t} + \dot{x}\frac{\partial f}{\partial x} + \dot{p}\frac{\partial f}{\partial p} = 0. \tag{2.14}$$

b) For any dynamical variable (i.e., any function $Q(x,p,t)$), the expectation value of Q can be computed by using either the quantum mechanical wave function ψ or the classical probability distribution f. More precisely, it can be

shown that:

$$< Q >_f = < Q >_\psi \{1 + O(e^{-2\omega t})\}. \qquad (2.15)$$

The verification of (2.14) is straightforward and will not be shown. To verify (2.15), imagine evaluating $< Q >_\psi$ for the special case in which Q is a product of x's and p's, in any order. When the derivative associated with any factor of p is carried out, three types of terms will arise: the derivative can act on either a subsequent x in the product, or it can operate on either the real or imaginary terms in the exponent of the wave function (2.9). In the first type of term the power of x is reduced by one, and in the second type the power is increased by one at the cost of an explicit factor of $e^{-2\omega t}$. For the third type the power is increased by one and no suppression factor is obtained. After all the derivatives are carried out, each power of x results in a factor of $e^{\omega t}$ when the expectation value is evaluated— thus, the terms of the third type dominate over the others by a factor of $e^{2\omega t}$. Furthermore, these terms of the third type reproduce precisely the calculation of $< Q >_f$. Finally, one notes that the most general quantum-mechanical operator Q can be written as a sum of operators of the form considered above.

The probability distribution $f(x, p, t)$ describes classical trajectories which roll from rest, starting at the peak of the potential. These classical trajectories can be parametrized by

$$x(t) = Ce^{\omega t}, \qquad (2.16)$$

where the parametrization insures the constraint between p and x which is implied by the δ-function in the probability distribution (2.13). The probability distribution for the constant C can then be determined from that for x:

$$P(C) = P(x)\frac{dx}{dC} = \sqrt{\frac{2}{\pi}}\frac{1}{b}e^{-2C^2/b^2}. \qquad (2.17)$$

Thus, at large times $x(t)$ is determined up to a random multiplicative constant which obeys a Gaussian probability distribution.

The physical interpretation of C can be clarified by writing it as $C \equiv \pm b\exp\{-\omega\tau\}$,

so

$$x(t) = \pm be^{\omega(t-\tau)}. \qquad (2.18)$$

The parameter τ clearly represents a time delay in the classical solution. The probability distribution for τ is given by

$$P(\tau) = 2P(C)\frac{dC}{d\tau} = 2\sqrt{\frac{2}{\pi}}\omega e^{-\omega\tau}\exp\{-2e^{-2\omega\tau}\}, \qquad (2.19)$$

where the factor of 2 is inserted because there are two values of C (C and $-C$) corresponding to each value of τ. A graph of this probability distribution is shown in Figure 2. Thus, at late times the particle obeys a classical trajectory, but the time at which it begins to roll down the potential energy hill is determined by quantum processes, and is described by a classical probability distribution.

The approximation of a quantum wave function by a classical probability distribution is not often discussed, but it is well known in the context of the standard theory of quantum tunneling. Consider a particle moving in one dimension, with a potential of the shape shown in Figure 3a. In the standard description, a particle placed at point A will tunnel to point B; it will then roll along a classical trajectory in the positive x-direction. Since the time of the tunneling is described by a probability distribution, the final state is described by a probability distribution of classical trajectories. Note that in the fully quantum-mechanical treatment of the tunneling problem, the particle can be described by an idealized unnormalizable wave function of the form shown in Figure 3b. This wave function decays exponentially in time, and describes a probability flux which extends to infinity. The probability density $|\psi|^2$ has a peak near A, drops sharply between A and B, and then behaves relatively smoothly to the right of B. Just as in our discussion of the upside-down harmonic oscillator, this wave function (to the right of B) is accurately approximated by a probability distribution of classical trajectories.

III. The Scalar Field in the Inflationary Universe

In the last section we described the behavior of an upside-down harmonic oscillator, a problem which has many important features in common with the problem which really

concerns us. In this section we will describe an idealized quantum field theory model which approximates the behavior of the scalar field in the new inflationary universe scenario. The model is a free field theory, and is therefore exactly soluble. It is of course not totally realistic, but we believe that it qualitatively describes the correct physics. Furthermore, we hope that it will serve as a valid zero order approximation to a more complicated calculational scheme in which the interactions are taken into account perturbatively.

The idealized model is based on three assumptions, which we will discuss one at a time.

Assumption 1: We assume that the space-time is described exactly by the de Sitter metric:

$$ds^2 = -dt^2 + e^{2\chi t}d\vec{x}^2, \tag{3.1}$$

where the expansion rate χ is related to the mass density ρ_0 of the false vacuum by

$$\chi = \sqrt{\frac{8\pi}{3}G\rho_0}, \tag{3.2}$$

where G denotes Newton's constant.

Thus, we are paying no attention to the approach to de Sitter space, but simply assuming that the space is de Sitter for all time. For comoving wavelengths which are short compared to the Hubble length before the onset of inflation, this inaccuracy in the treatment of the metric should have very little effect— wavelengths which are very short compared to the Hubble length evolve in any case as if they were in Minkowski space. However, we must remember that the longest wavelengths-- those which are comparable to or larger than the Hubble length at the onset of inflation-- are not being treated accurately.

By using Assumption 1, we are also ignoring the fluctuations of the metric which result from the fluctuations of the matter fields.

We will consider a single scalar field evolving in this idealized de Sitter space. Such a field can be described by an action

$$S = \int d^4x\sqrt{g}\left\{-\frac{1}{2}g^{\mu\nu}\partial_\mu\phi\partial_\nu\phi - V(\phi)\right\}, \tag{3.3}$$

where the potential $V(\phi)$ is given by

$$V(\phi) = \frac{1}{4}\lambda\left(\phi^2 - \frac{\mu^2}{\lambda}\right)^2. \tag{3.4}$$

For pedagogical purposes we are setting c and k (Boltzmann constant) equal to one, but in Sections III-V we will keep factors of $\hbar$. It is then necessary to specify, for example, whether μ denotes a mass or an inverse length. We make this choice according to the usual prescription that S should represent the action of a classical field theory, and the quantity $\hbar$ should not appear until the classical theory is quantized. S must therefore have the units of $mass \times length$, from which it follows that ϕ has units of $mass^{1/2} \times length^{-1/2}$, μ has units $length^{-1}$, and λ has units $mass^{-1} \times length^{-1}$. Note that $\hbar\lambda$ is then dimensionless.

A plot of this potential is shown as Figure 4. The potential has a minimum at

$$\phi_c = \frac{\mu}{\sqrt{\lambda}}. \tag{3.5}$$

The false vacuum energy density is given by

$$\rho_0 = \frac{\mu^4}{4\lambda}, \tag{3.6}$$

leading to a de Sitter expansion rate

$$\chi = \sqrt{\frac{2\pi G}{3\lambda}}\mu^2. \tag{3.7}$$

Using the metric (3.1), the action can be written out more explicitly as

$$S = \int d^4x\mathcal{L}, \tag{3.8a}$$

where the Lagrangian density is given by

$$\mathcal{L} = e^{3\chi t}\left\{\frac{1}{2}\dot{\phi}^2 - \frac{1}{2}e^{-2\chi t}(\vec{\nabla}\phi)^2 + \frac{1}{2}\mu^2\phi^2 - \frac{1}{4}\lambda\phi^4 - \frac{\mu^4}{4\lambda}\right\}. \tag{3.8b}$$

The equations of motion are then

$$\ddot{\phi} + 3\chi\dot{\phi} - e^{-2\chi t}\vec{\nabla}^2\phi = \mu^2\phi - \lambda\phi^3. \tag{3.9}$$

To quantize this system, we will use standard canonical techniques, which are totally equivalent to the path integral techniques which might otherwise be employed. (Note that the dynamics of quantized fields in curved space is straightforward. The subtleties, which we will confront later, involve such questions as the nature of the "vacuum" state.) Thus we introduce a canonical momentum density

$$\pi(\vec{x}) = \frac{\partial \mathcal{L}}{\partial\dot{\phi}(\vec{x})} = e^{3\chi t}\dot{\phi}, \tag{3.10}$$

and impose the canonical equal-time commutation relations

$$[\phi(\vec{x},t), \pi(\vec{y},t)] = i\hbar\delta^3(\vec{x}-\vec{y}). \tag{3.11}$$

The theory we have so far constructed is an interacting quantum field theory, which is certainly not exactly soluble. Assuming that λ is sufficiently small, however, one would expect that the interacting theory can be accurately described by perturbation theory. At nonzero temperature, however, one must be careful in choosing the proper free field theory to use as a zero order approximation. Consider what happens, for example, if the quantum field theory of Eqs. (3.3) and (3.4) is formulated in flat space at nonzero temperature. If one develops a perturbation expansion which begins with the free field theory obtained by simply neglecting λ, then one finds that loop integrations give rise to terms proportional to $\hbar\lambda T^2/(\hbar\mu)^2$. Thus, naive perturbation theory becomes invalid when $T \gtrsim \hbar\mu/\sqrt{\hbar\lambda}$. However, S. Weinberg[28] has shown that the validity of perturbation theory for this range of temperatures can be restored by modifying the mass term of the zero order potential to give

$$V_0(\phi) = -\frac{1}{2}\left(\mu^2 - \frac{\lambda T^2}{4\hbar}\right)\phi^2. \tag{3.12}$$

Of course one cannot change the actual mass, so the mass correction term $\lambda T^2\phi^2/8\hbar$ must be compensated by the introduction of a new counterterm $-\lambda T^2\phi^2/8\hbar$. Terms

proportional to this counterterm then appear in higher orders of perturbation theory, and they serve to precisely cancel the leading thermal corrections which arise at high temperature. In this approximation the model will undergo a phase transition when the sign of the effective mass term changes, at a critical temperature

$$T_c = 2\mu\sqrt{\hbar/\lambda}. \tag{3.13}$$

(In the language of other authors[29], the extra term in Eq. (3.12) is the leading term in the finite temperature effective potential. For our present purposes, however, the logic used by Weinberg seems the most useful.) Note that thermal effects are enhanced as $\hbar \to 0$, reflecting the divergences that exist in the classical statistical mechanics of field theories (Rayleigh-Jeans theory).

In the high temperature regime ($T \gg \hbar\chi$), the complications of de Sitter space corrections are insignificant and the analysis of Weinberg applies. In this regime it is also true that RT =constant, which leads us to our next assumption:

> **Assumption 2:** The potential energy function will be taken as expression (3.12), where
>
> $$T = T_0 e^{-\chi t}. \tag{3.14}$$

Note that the value of T_0 has no physical significance— it is simply the value of the temperature at the arbitrary time $t = 0$.

We expect Assumption 2 to be accurate for the high temperature regime. When T becomes comparable to $\hbar\chi$, however, the interparticle spacing becomes comparable to the de Sitter horizon distance[30] χ^{-1}, and the notion of thermal equilibrium ceases to make sense. Fortunately, at this point the thermal correction in Eq. (3.12) is no longer large enough to be significant, so it does not matter if it is calculated accurately or not. Thus, we consider the assumption valid for its intended purpose.

Assumption 2 excludes the possibility that the zero-temperature effective potential contains significant quantum corrections, and it therefore excludes potentials of the Coleman-

Weinberg[12] type. However, by studying the case $\mu^2 = 0$ in our model one can at least learn about the initial behavior of fluctuations in Coleman-Weinberg models. We hope that in the future we will be able to treat this case in more detail.

The dynamics of our model system has now been completely defined, and our one remaining assumption will specify the nature of the initial state. It is here that questions about the nature of the de Sitter space "vacuum" will arise. However, before we can describe this last assumption, it is necessary to develop the description of the dynamics in more detail.

Since the problem has been reduced to a free field theory, we can use a Fourier decomposition in order to obtain decoupled degrees of freedom. In order to keep the analogy with the upside-down harmonic oscillator of Section II as close as possible, we will expand in sine and cosine functions rather than in complex exponentials, so that the expansion coefficients will be real. Furthermore, we will begin by imagining that our system is confined to a cubic box with periodic boundary conditions, with the coordinate length of each side fixed at a value b — the Fourier decomposition is then a discrete sum. The limit $b \to \infty$ can be taken at the end. Thus we write

$$\phi(\vec{x},t) = \frac{1}{(2\pi)^{3/2}}\left(\frac{2\pi}{b}\right)^3 \left\{\sqrt{2}\sigma(\vec{0},t) + \sum_{\substack{\vec{k}=(\frac{2\pi}{b})\vec{n} \\ \vec{n}\ \text{integer} \\ \vec{n}\neq 0}} \left[\sigma_+(\vec{k},t)\cos\vec{k}\cdot\vec{x} + \sigma_-(\vec{k},t)\sin\vec{k}\cdot\vec{x}\right]\right\}, \tag{3.15}$$

where

$$\sigma_+(-\vec{k},t) \equiv \sigma_+(\vec{k},t)$$

and

$$\sigma_-(-\vec{k},t) \equiv -\sigma_-(\vec{k},t).$$

Note that the zero-momentum mode lacks the $\vec{k} \to -\vec{k}$ redundancy exhibited by all other modes, and it therefore requires special treatment. The normalization used for the zero-momentum mode has been chosen to simplify the subsequent equations.

It can be seen already that the expansion in sines and cosines is both unfamiliar and a bit awkward. We will proceed with it nonetheless, because we think that the analogy with the upside-down harmonic oscillator is conceptually very important. However, in Appendix A we will translate our results into the language of the usual expansion in complex exponentials.

To simplify our notation, we denote the mode variables $\sigma(\vec{0},t)$ and $\sigma_\pm(\vec{k},t)$ generically by $\sigma_\alpha(t)$. Whenever α is summed, we adopt the convention that the sum includes the zero momentum mode, and also one entry of σ_+ and one entry of σ_- for each pair $(\vec{k},-\vec{k})$.

Since we have reduced the problem to a free field theory, the mode variables $\sigma_\alpha(t)$ will completely decouple from each other. Thus we can study the quantum mechanics of these mode variables one at a time, and each variable σ_α will be treated in a manner which is analogous to the treatment of the variable x of the upside-down harmonic oscillator. However, although the underlying physics in the two problems is very similar, the problem of the σ_α's is somewhat more difficult— the time-dependence is more complicated, and in this case we will want to extend our understanding to include thermal ensembles of states. It will therefore be useful to use a formalism based on creation and annihilation operators, very similar to those used in the conventional treatment of the ordinary harmonic oscillator. A discussion completely parallel to the one-dimensional quantum-mechanical case is given in Appendix B, using the functional-Schrödinger picture of field theory.

When the expansion (3.15) is inserted into the Lagrangian of Eq. (3.8), one obtains

$$L = \left(\frac{2\pi}{b}\right)^3 e^{3\chi t} \sum_\alpha \left\{\dot{\sigma}_\alpha^2 + \left[\mu^2 - e^{-2\chi t}\left(\vec{k}_\alpha^{\,2} + \gamma^2\right)\right]\sigma_\alpha^2\right\}, \tag{3.16}$$

where

$$\gamma^2 = \frac{\lambda T_0^2}{4\hbar}. \tag{3.17}$$

The equation of motion for each mode variable is then given by

$$\ddot{\sigma}_\alpha + 3\chi\dot{\sigma}_\alpha = \left[\mu^2 - e^{-2\chi t}\left(\vec{k}_\alpha^{\,2} + \gamma^2\right)\right]\sigma_\alpha. \tag{3.18}$$

The two linearly independent solutions to this second order equation are found to be

$$\sigma_\alpha(t) \propto e^{-\frac{3}{2}\chi t}\begin{cases} J_p(z) \\ N_p(z), \end{cases} \tag{3.19}$$

where

$$p = \sqrt{\frac{9}{4} + \frac{\mu^2}{\chi^2}}, \tag{3.20}$$

$$z = \frac{\sqrt{\vec{k}_\alpha^2 + \gamma^2}}{\chi} e^{-\chi t}, \tag{3.21}$$

and $J_p(z)$ and $N_p(z)$ denote the Bessel functions of the first and second kind, respectively. Some useful properties of these functions are tabulated in Appendix C.

The Lagrangian (3.16) is quantized canonically. One introduces a canonical momentum conjugate to each mode variable σ_α:

$$\pi_\alpha = \frac{\partial L}{\partial \dot{\sigma}_\alpha} = 2\left(\frac{2\pi}{b}\right)^3 e^{3\chi t}\dot{\sigma}_\alpha. \tag{3.22}$$

The Hamiltonian is then given by

$$\begin{aligned} H &= \sum_\alpha \pi_\alpha \dot{\sigma}_\alpha - L \\ &= \sum_\alpha \left\{ \frac{1}{4}\left(\frac{b}{2\pi}\right)^3 e^{-3\chi t}\pi_\alpha^2 + \left(\frac{2\pi}{b}\right)^3 e^{3\chi t}\left[e^{-2\chi t}\left(\vec{k}_\alpha^2 + \gamma^2\right) - \mu^2\right]\sigma_\alpha^2 \right\}. \end{aligned} \tag{3.23}$$

One then imposes the canonical commutation relations

$$[\sigma_\alpha, \pi_{\alpha'}] = i\hbar\delta_{\alpha',\alpha}. \tag{3.24}$$

In order to describe our initial state assumption, it is necessary to first describe the behavior of this quantum system for early times. The mode variable $\sigma_\alpha(t)$ describes a perturbation of physical wavelength $(2\pi/k_\alpha)e^{\chi t}$, and thus for sufficiently early times the wavelength is very small compared to the de Sitter horizon distance χ^{-1}. At such short distance scales, however, **de Sitter space is indistinguishable from Minkowski space.** In fact, one could imagine that our universe has a small positive cosmological constant, and that today it is just beginning a de Sitter phase. The de Sitter horizon distance would then be on the order of 10^{10} light years. While such a cosmological situation would have important implications for the ultimate fate of the universe, it would have absolutely no detectable effect on particle physics experiments done at Fermilab— because

those experiments are sensitive only to wavelengths much shorter than the de Sitter horizon distance.

The flat-space behavior of short wavelengths in de Sitter space can be seen in Eqs. (3.16), (3.18), or (3.23), which indicate that at early times each mode function σ_α behaves like a harmonic oscillator, with frequency

$$\omega(t) = e^{-\chi t}\sqrt{\vec{k}_\alpha^2 + \gamma^2}. \tag{3.25}$$

Although the frequency varies on the time scale of χ^{-1}, for early times $\omega \gg \chi$ and thus the change in frequency is adiabatic. Thus, one expects that the solutions to the differential equation (3.18) should behave sinusoidally for very early times, except that the frequency will slowly shift. If the Bessel functions in Eq. (3.19) are taken in the linear combination of the Hankel functions (see Eq. (C.1)), then these sinusoids become complex exponentials. The behavior of the Hankel functions for asymptotically large z is given by Eq. (C.2). Then if $z(t)$ is expanded for $t \approx t_0$ for some early value of t_0 ("early" is defined by $z(t_0) \gg 1$), one has

$$H_p^{(k)}(z) \propto e^{\mp i\omega(t)(t-t_0)}, \tag{3.26}$$

where the expansion for $z(t)$ is valid provided that $|\chi(t-t_0)| \ll 1$.

Motivated by the above arguments about flat-space behavior at early times, we rewrite the mode variables $\sigma_\alpha(t)$ in terms of mode functions $\psi(\vec{k}_\alpha, t)$. These mode functions are exact solutions to the equation of motion (3.18), and at asymptotically early times they approach the same complex exponential functions that one would use in the analogous flat-space calculation. Thus one writes

$$\sigma_\alpha(t) = \frac{1}{\sqrt{2}}\left(\frac{b}{2\pi}\right)^{3/2}\left[a_\alpha\psi(\vec{k}_\alpha, t) + a_\alpha^\dagger\psi^*(\vec{k}_\alpha, t)\right], \tag{3.27}$$

where

$$\psi(\vec{k}, t) \equiv \frac{1}{2}\sqrt{\frac{\pi\hbar}{\chi}}e^{-\frac{3}{2}\chi t}H_p^{(1)}(z), \tag{3.28}$$

and the a_α are operators which are defined by Eq. (3.27). The relationship can then be inverted by using the identity (C.4), from which it follows that

$$\psi\frac{\partial\psi^*}{\partial t} - \frac{\partial\psi}{\partial t}\psi^* = i\hbar e^{-3\chi t}. \tag{3.29}$$

Carrying out the inversion gives

$$a_\alpha = \frac{\sqrt{2}}{i\hbar}\left(\frac{2\pi}{b}\right)^{3/2} e^{3\chi t}\left[\frac{\partial\psi^*}{\partial t}\sigma_\alpha - \psi^*\frac{\partial\sigma_\alpha}{\partial t}\right]. \tag{3.30}$$

The canonical commutation relations (3.24) can then be used to show that

$$\begin{aligned}[a_\alpha, a^\dagger_{\alpha'}] &= \delta_{\alpha',\alpha} \\ [a_\alpha, a_{\alpha'}] &= 0.\end{aligned} \tag{3.31}$$

Thus, at early times one can think of the operators $a^\dagger_\alpha$ and a_α as creation and annihilation operators for one-particle (standing wave) states with properties which are indistinguishable from the usual properties of Minkowski space quantum field theory. (Of course the commutation relations (3.31) hold at late times as well, but the one-particle interpretation has to be abandoned because the time-dependence of the mode functions becomes more complicated.)

We then specify the initial state of the system by the following assumption:

> **Assumption 3:** At asymptotically early times, when each mode behaves like a simple harmonic oscillator, we assume that the system can be described by a density matrix corresponding to thermal equilibrium at the background temperature $T = T_0 e^{-\chi t}$.

Note that although the temperature T is changing with time, it is not necessary to pick any particular time at which to fix our initial thermal ensemble. According to Eq. (3.25), the oscillator frequency $\omega(t)$ is also falling as $e^{-\chi t}$, so the ratio ω/T behaves as a constant at asymptotically early times. Since the thermal equilibrium density matrix depends only on this ratio, it is possible to maintain thermal equilibrium at all asymptotically early times.

Note also that if the temperature T_0 in Assumption 3 were set equal to zero, so that each oscillator were put into its ground state, then the resulting state would be the standard de Sitter space "vacuum"- the one which is used in the papers by Gibbons and Hawking[31] or Bunch and Davies[32]. Thus, the thermal effects of the Gibbons-Hawking temperature $\chi/2\pi$ are taken into account implicitly by our formalism. (Although the logic

used in our construction makes no mention of the full de Sitter group, it can be shown[32] that the symmetry is manifested in the propagator, and therefore in all Green's functions.)

Although we regard Assumption 3 to be as plausible as any assumption about the initial state, we must point out that it is not necessarily true. For the very small values of λ which will be necessary in order to obtain a reasonable spectrum of density fluctuations (see Section VII), the interactions are far too weak to cause thermalization in the time available.[33] Thus, thermal equilibrium is really only one of many conceivable initial states. It is clear, of course, that sufficient inflation will always wipe out the memory of the initial state, since the wavelengths which are relevant at late times corresponded in the early universe to such extremely high energies that only the zero-point oscillations could have been excited. However, questions such as the duration of inflation are sensitive to arbitrarily long wavelengths, and are affected by the initial state. Thus, it would be worthwhile to explore the consequences of other initial states, but we have not yet done so.

Now that both the dynamics and the initial state have been specified, it is just a matter of straightforward calculation to answer any question that one might ask about the behavior of this idealized model. Using Assumption 3, the expectation values of products of the operators a_α and $a^\dagger_\alpha$ can be calculated by using the results for a canonical ensemble of a simple harmonic oscillator. In particular, one has

$$< a^\dagger_{\alpha'} a_\alpha > = \frac{1}{e^{\Theta_\alpha} - 1}\delta_{\alpha'\alpha}, \tag{3.32a}$$

where

$$\Theta_\alpha \equiv \lim_{t\to-\infty}\frac{\hbar\omega(t)}{T(t)} = \frac{\hbar}{T_0}\sqrt{k_\alpha^2 + \gamma^2}. \tag{3.32b}$$

One also has

$$< a_{\alpha'} a_\alpha > = < a^\dagger_{\alpha'} a^\dagger_\alpha > = 0. \tag{3.32c}$$

Using (3.27), we can similarly calculate expectation values involving the σ_α's. There is no correlation between different values of α, and one has

$$< \sigma_\alpha(t) > = 0, \tag{3.33}$$

and

$$< \sigma_\alpha^2(t) >= \frac{1}{2}\left(\frac{b}{2\pi}\right)^3 |\psi(\vec{k}_\alpha, t)|^2 \coth\left(\tfrac{1}{2}\Theta_\alpha\right), \tag{3.34}$$

where $\psi(\vec{k}_\alpha, t)$ was defined in Eq. (3.28). The behavior of $|\psi(\vec{k}_\alpha, t)|^2$ and $\coth\left(\frac{1}{2}\Theta_\alpha\right)$ are shown in Figure 5.

It is interesting to examine the appearances of $\hbar$ in Eq. (3.34). If one takes $T_0 = 0$, then the right-hand-side is proportional to $\hbar$ (which is contained in the definition (3.28) of $\psi(\vec{k}, t)$)— in this case one is seeing pure quantum fluctuations. If one takes $T_0 \neq 0$ and γ^2 fixed, then $\hbar$ disappears in the limit $\hbar \to 0$ — in this case one is seeing classical thermal fluctuations for a given mode. The quantity γ^2, on the other hand, arises from a sum over modes; the Rayleigh-Jeans divergence of classical field theory causes it to diverge as $\hbar \to 0$, as can be seen in Eq. (3.17).

The expectation value of arbitrary powers of $\sigma_\alpha(t)$ can also be calculated by using standard harmonic oscillator techniques— the problem is identical to finding finite temperature expectation values of powers of a harmonic oscillator coordinate x. It can be shown[34] that under these circumstances x obeys a Gaussian probability distribution, and therefore the same applies to $\sigma_\alpha(t)$. The probability distribution is therefore completely determined by its mean and variance, specified by Eqs. (3.33) and (3.34). (In the infinite volume limit, however, the probability distribution for a single mode becomes irrelevant. The number of modes which enter the sum which determines $\phi(\vec{x}, t)$ approaches infinity, and the central limit theorem implies that the probabilities become Gaussian. All that matters is the variance of the probability distribution for each $\sigma_\alpha(t)$, and the fact that they are independent.[35])

The expression for $< \sigma_\alpha^2(t) >$ can be made more explicit in the special case of $\mu^2 = 0$, in which case $p = 3/2$ and a simple closed form expression exists for $H_p^{(1)}(z)$ (see Eq. (C.5)). One then has

$$< \sigma_\alpha^2(t) >= \frac{1}{4}\left(\frac{b}{2\pi}\right)^3 \frac{\hbar\chi^2}{\left(\vec{k}_\alpha^2 + \gamma^2\right)^{3/2}}\left[1 + \frac{\vec{k}_\alpha^2 + \gamma^2}{\chi^2} e^{-2\chi t}\right] \coth\left(\tfrac{1}{2}\Theta_\alpha\right). \tag{3.35}$$

It is now possible to calculate expectation values for arbitrary products of fields $\phi(\vec{x}, t)$.

It will be particularly useful to have an expression for the equal-time propagator, which in the infinite volume limit is given by

$$< \phi(\vec{x}, t)\phi(\vec{y}, t) >= \frac{1}{(2\pi)^3} \int d^3\vec{k}\, e^{i\vec{k}\cdot(\vec{x}-\vec{y})} |\psi(\vec{k}, t)|^2 \coth\left(\tfrac{1}{2}\Theta_{\vec{k}}\right). \tag{3.36}$$

The reader who wishes to derive the above equation will find some useful intermediate steps in Appendix A. For the special case of $\mu^2 = 0$ the expression reduces to

$$\begin{aligned} < \phi(\vec{x}, t)\phi(\vec{y}, t) >= \frac{\hbar\chi^2}{16\pi^3} \int d^3\vec{k}\, e^{i\vec{k}\cdot(\vec{x}-\vec{y})} \frac{1}{(\vec{k}^2 + \gamma^2)^{3/2}} \\ \times \left[1 + \frac{\vec{k}^2 + \gamma^2}{\chi^2} e^{-2\chi t}\right] \coth\left(\frac{\hbar\sqrt{\vec{k}^2 + \gamma^2}}{2T_0}\right). \end{aligned} \tag{3.37}$$

IV. Classical Behavior at Late Times

Following the logic described in Sec. II, at late times we can think of each Fourier coefficient $\sigma_\alpha(t)$ as a classical variable with a value described by a classical probability distribution. Once the classical approximation becomes valid, one can use classical equations of motion to describe the subsequent evolution.

To see when the classical approximation becomes valid, we should check to see when the minimal quantum uncertainty $(\Delta\sigma_\alpha\, \Delta\pi_\alpha)_{\min} = \frac{1}{2}\hbar$ becomes negligible. More precisely, we must see when the ratio

$$R_\alpha = \frac{\sqrt{< \sigma_\alpha^2 >< \pi_\alpha^2 >}}{(\Delta\sigma_\alpha\, \Delta\pi_\alpha)_{\min}} \tag{4.1}$$

becomes much larger than one. To calculate R_α at late times, one begins by rewriting Eq. (3.34), using Eq. (C.3) to describe the asymptotic form of the Bessel functions appearing in $\psi(\vec{k}_\alpha, t)$, as defined by Eq. (3.28). One obtains the asymptotic form

$$\begin{aligned} < \sigma_\alpha^2(t) > \xrightarrow[t \to \infty]{} \left(\frac{b}{2\pi}\right)^3 \frac{\hbar}{8\pi\chi} e^{(2p-3)\chi t} \Gamma^2(p) \\ \times \left[\frac{4\chi^2}{\vec{k}_\alpha^2 + \gamma^2}\right]^p \coth\left(\tfrac{1}{2}\Theta_\alpha\right). \end{aligned} \tag{4.2}$$

It is easily seen that the growth factor $e^{(2p-3)\chi t}$ agrees with the asymptotic classical growth rate for solutions to the differential equation (3.9), ignoring the $\lambda\phi^3$ interaction term. One can carry out an analogous calculation of $< \dot{\sigma}_\alpha^2 >$, which is related to $< \pi_\alpha^2 >$ by Eq. (3.22). Finally, one obtains

$$R_\alpha \xrightarrow[t\to\infty]{} \frac{(2p-3)\Gamma^2(p)}{\pi}\left(\frac{z}{2}\right)^{-2p}\coth\left(\tfrac{1}{2}\Theta_\alpha\right). \tag{4.3}$$

Thus it is clear that for z sufficiently small (t sufficiently large), the desired criterion is met. Note that z can be thought of as the ratio of the horizon length χ^{-1} to the "effective wavelength" $2\pi e^{\chi t}/\sqrt{\vec{k}_\alpha^2+\gamma^2}$, so the behavior of $\sigma_\alpha(t)$ can be described classically whenever the effective wavelength is much larger than the horizon length.

The special case of $\mu^2 = 0$ must be treated separately, since in this case $p = \frac{3}{2}$ and the right hand side of Eq. (4.3) vanishes identically. Repeating the calculation, one finds that the leading term in this case gives

$$R_\alpha \xrightarrow[t\to\infty]{} \frac{1}{z}\coth\left(\tfrac{1}{2}\Theta_\alpha\right). \tag{4.4}$$

R_α does not grow as quickly in this case, but it is still true that the behavior is classical whenever the effective wavelength is much larger than the horizon length.

V. The Smeared Field Operator

Since we know the probability distribution for each coefficient σ_α which occurs in the expansion (3.15) for the scalar field $\phi(\vec{x})$, one might think that the probability distribution for the field itself is well determined. This is basically true, but there is one subtlety which must still be taken into account. If one were to calculate $< \phi^2(\vec{x},t) >$ using the probability distribution described above, one would find that the sum over modes would diverge at large $\vec{k}$. Thus there are infinite fluctuations in $\phi(\vec{x},t)$, in the sense that the standard deviation of the probability distribution is infinite.

In fact, whenever one tries to discuss the value of a quantum field at a specified point, whether in flat or curved space-time, the fluctuations in the field are always infinite. Unlike many other infinities which arise in quantum field theory calculations, this infinity

is physically real and should **not** be removed by a renormalization. It means that if one were to measure the field with a device which has a spatial resolution ℓ, then the width of the probability distribution for the measured value of the field would increase without bound as ℓ becomes smaller and smaller.

A measurable quantity with finite fluctuations can be defined by "smearing" the field in a manner which simulates the finite spatial resolution of a measuring device, so that its value corresponds to a spatial average of the local quantum field $\phi(\vec{x})$. For definiteness, we will use smeared fields which are defined with a Gaussian weight function:

$$\hat{\phi}_\ell(\vec{x},t) = \frac{1}{(2\pi)^{\frac{3}{2}}\ell^3}\int d^3\vec{y}\, e^{-\frac{1}{2}(\vec{x}-\vec{y})^2/\ell^2}\phi(\vec{y},t), \tag{5.1}$$

where ℓ is an arbitrary smearing length. Using the expansion (3.15) for the scalar field operator $\phi(\vec{x},t)$, one obtains a rather simple expansion for the smeared field operator $\hat{\phi}_\ell(\vec{x},t)$:

$$\hat{\phi}_\ell(\vec{x},t) = \frac{1}{(2\pi)^{3/2}}\left(\frac{2\pi}{b}\right)^3\left\{\sqrt{2}\sigma(\vec{0},t) + \sum_{\substack{\vec{k}=(\frac{2\pi}{b})\vec{n}\\ \vec{n}\ \text{integer}\\ \vec{n}\neq 0}} e^{-\frac{1}{2}\vec{k}^2\ell^2}\left[\sigma_+(\vec{k},t)\cos\vec{k}\cdot\vec{x} + \sigma_-(\vec{k},t)\sin\vec{k}\cdot\vec{x}\right]\right\}. \tag{5.2}$$

Thus, the smearing can be seen to provide precisely the sort of high $|\vec{k}|$ cutoff which is required.

The probability distribution for the field $\hat{\phi}_\ell(\vec{x},t)$ is then perfectly well defined. If one wishes to visualize a typical configuration for the the scalar field at any point in its evolution, one can use Monte Carlo techniques to generate values for each of the σ_α according to a Gaussian probability distribution of the correct width. At present we are developing a computer program to carry out this procedure. One can also calculate $< \dot{\hat{\phi}}_\ell^2(t) >$, which is given in the infinite volume limit (see Appendix A for useful intermediate steps) by

$$< \dot{\hat{\phi}}_\ell^2(\vec{x},t) > = \frac{H}{8\pi\chi}e^{-3\chi t}\int_0^\infty k^2\, dk\, e^{-k^2\ell^2} \qquad \times$$

$$\times [J_p^2(z) + N_p^2(z)] \coth\left(\frac{\hbar\sqrt{k^2+\gamma^2}}{2T_0}\right), \tag{5.3}$$

where γ, p, and z are given by Eqs. (3.17), (3.20), and (3.21).

VI. Numerical Results

In this section we will present some numerical results based on the formulas derived in the previous section. For convenience we will now set $\hbar = 1$, and we introduce the notation $G \equiv 1/M_P^2$, where $M_P = 1.22 \times 10^{19}$ GeV denotes the Planck mass.

The Lagrangian for the scalar field is contained in Eqs. (3.3) and (3.4), and involves the two free parameters λ and μ. It is however more convenient to think in terms of dimensionless parameters, which can be taken as λ and $\eta \equiv \mu^2/\chi^2$. The original parameter μ can then be recovered by rewriting Eq. (3.7) as

$$\mu = \sqrt{\frac{3\lambda}{2\pi\eta}} M_P. \tag{6.1}$$

In order for the mass density fluctuations to be sufficiently small, as will be discussed in the next section, it is necessary for λ to be very small— of order 10^{-12}. Thus we will be primarily concerned with values of λ in this vicinity. The value of η is very important to the estimation of the duration of the inflationary era— the larger the value of η, the more unstable is the false vacuum configuration. We will explore values of η in the range of 0.1 to 10. Note that ϕ_o (the value of ϕ which minimizes the potential) is then given by

$$\phi_o = \sqrt{\frac{3}{2\pi\eta}} M_P, \tag{6.2}$$

and that

$$T_c = 2\phi_o, \tag{6.3}$$

and

$$\chi = \frac{1}{\eta}\sqrt{\frac{3\lambda}{2\pi}} M_P. \tag{6.4}$$

Thus, for the purely scalar model, both ϕ_c and T_c tend to be of order of the Planck scale, and can be somewhat larger than Planck scale when η is small. The smearing length ℓ is not a parameter of the physical problem, but it is a parameter of the questions that we

will be asking. We will usually take $\ell = T_0^{-1}$, so the smearing length will correspond to one thermal wavelength.

Figure 6 shows how $\hat{\phi}_\ell^{RMS} \equiv < \hat{\phi}_\ell^2 >^{1/2}$ varies with time, for $\eta = 0.2$ and $\lambda = 10^{-12}$. The zero of time for this figure has been fixed by setting $T_0 \equiv \chi$, and the smearing length has been chosen as $\ell = T_0^{-1}$. The point where $\phi = \phi_c$ is labelled A, the point where $T = T_c$ is labelled B, and the point where $T = \chi$ is labelled D.

The graph has been drawn using our approximation of a perfect de Sitter space for all time, but it is interesting to mark on the graph the time at which de Sitter expansion is actually expected to begin. This will occur roughly when the false vacuum energy ρ_0, defined by Eq. (3.6), is equal to the thermal energy density, which is given by

$$\rho_{th} = \frac{\pi^2}{30} N_{eff} T^4, \tag{6.5}$$

where N_{eff} denotes the effective number of massless spin degrees of freedom (i.e., each bosonic spin state with mass $\ll T$ counts as one unit, and each fermionic spin state with mass $\ll T$ counts as 7/8). Thus $\rho_0 = \rho_{th}$ at a temperature T_{deS} given by

$$T_{deS} = \frac{3}{2\pi\eta^{1/2}}\left(\frac{10\lambda}{3N_{eff}}\right)^{1/4} M_P. \tag{6.6}$$

The value of T_{deS} is shown on Figure 6 as point C, using the estimate $N_{eff} \approx 200$. At first one might be worried, since the point $T = T_{deS}$ is not at the extreme left of the graph. However, most of the thermal excitations occur at wavelengths of order T^{-1}, and at early times they behave in any case as if they were in Minkowski space. The non-Minkowski nature of the space becomes important when $T \approx \chi$, when these wavelengths cross the de Sitter horizon (which occurs at $t \approx 0$ in Figure 6). Since $T_{deS} \gg \chi$, the universe has by this time been undergoing de Sitter expansion for many time constants (χ^{-1}). Excitations of the longest wavelengths will of course be strongly influenced by the non-de Sitter behavior at early times, but we will not consider this effect.

Note that Figure 6 provides a clear answer, at least in the context of our assumptions, to the first question mentioned in the introduction. According to the picture described by Mazenko, Unruh, and Wald,[11] when T falls below T_c the scalar field is expected to settle

into small regions with $\phi \approx \pm\phi_c$. The expected size of these regions would be of order T^{-1}, which is exactly the smearing length used in Figure 6. Thus, if this picture were valid, then $\hat{\phi}_\ell^{RMS}$ would level off at a value of order ϕ_c when T fell to T_c. As can be seen in Figure 6, the actual behavior of $\hat{\phi}_\ell^{RMS}$ is very different. $\hat{\phi}_\ell^{RMS}$ continues to fall long after T reaches T_c, decreasing to a value many orders of magnitude below ϕ_c.

The continued falling of $\hat{\phi}_\ell^{RMS}$ is a clear result of our numerical calculations, and the reason can be easily understood. When $T \approx T_c$, fluctuations will indeed carry $\hat{\phi}_\ell^{RMS}$ to values of order $\pm\phi_c$. However, when one decomposes these fluctuations into Fourier components as in Eq. (5.3), one sees that they are dominated by wavelengths of order T^{-1}. For these wavelengths

$$k^2_{\rm physical} \equiv e^{-2\chi t}k^2 \approx T^2 \approx \frac{4\mu^2}{\lambda} \gg \mu^2, \tag{6.7}$$

so the fact that the potential energy function is unstable is irrelevant to these modes— they continue to evolve for some time like the modes of a massless free field. And for a massless free field, dimensional analysis guarantees that $\hat{\phi}_\ell^{RMS} \propto T$. Note that this argument depends on the condition $\lambda \ll 1$; if λ were of order one, then the picture of Mazenko, Unruh, and Wald would presumably be a valid description.

It is clearly seen in Figure 6 that $\hat{\phi}_\ell^{RMS}$ traces out straight lines for both early and late times, with a short segment of curve which interpolates between the two asymptotic lines. Expressions for these two asymptotic lines are derived in Appendix D, but we state the results here. For early times one has

$$\hat{\phi}_\ell^{RMS} \to T_0 e^{-\chi t} F(\lambda, T_0\ell), \tag{6.8a}$$

where

$$F^2(\lambda, T_0\ell) = \frac{1}{16\pi^2}\int_0^\infty dy\, \frac{y^2}{\sqrt{y^2+\lambda}} e^{-(T_0\ell y)^2/4} \times \coth\left(\frac{1}{4}\sqrt{y^2+\lambda}\right). \tag{6.8b}$$

$F(\lambda, T_0\ell)$ has a smooth limit as $\lambda \to 0$, and numerically one finds, for example, that

$F(0,1) = 0.215$. For late times we find

$$\hat{\phi}_\ell^{RMS}(t) \to \chi\left[\frac{\chi}{T_0}e^{\chi t}\right]^{p-\frac{3}{2}} \tilde{F}(\lambda, \eta, T_0\ell), \tag{6.9a}$$

where

$$\tilde{F}^2(\lambda, \eta, T_0\ell) = \frac{\Gamma^2(p)}{\pi^3}\left(\frac{4}{\sqrt{\lambda}}\right)^{2p-3} \times \int_0^\infty dy \frac{y^2}{(y^2+1)^p} e^{-\lambda(T_0\ell y)^2/4} \coth\left(\frac{1}{4}\sqrt{\lambda(y^2+1)}\right), \tag{6.9b}$$

where as before $p = \frac{1}{2}\sqrt{9+4\eta}$. $\tilde{F}(\lambda, \eta, T_0\ell)$ does not behave smoothly as $\lambda \to 0$, but rather behaves as

$$\tilde{F}^2(\lambda, \eta, T_0\ell) \sim \frac{\Gamma^2(p)}{\pi^{5/2}\sqrt{\lambda}(p-1)\Gamma(p+\frac{1}{2})}\left(\frac{4}{\sqrt{\lambda}}\right)^{2p-3}. \tag{6.10}$$

Note that the leading behavior above is independent of $T_0\ell$— for very small λ, the field ϕ at large times is apparently very smooth on comoving scales ℓ of order T_0^{-1}, and so the smearing length does not matter.

It is shown in Appendix D that the behavior of $\hat{\phi}_\ell^{RMS}$ at large times (Eqs. (6.9)) is dominated by wavelengths which are of order $1/\sqrt{\lambda}$ times the thermal wavelength T^{-1}. Thus these dominant wavelengths cross the de Sitter horizon when $T \approx \chi/\sqrt{\lambda} \approx M_P/\eta$ (where we used Eq. (6.4) for χ). Since this temperature is higher than the temperature T_{deS} at which de Sitter expansion is expected to actually begin, it follows that our assumption of exact de Sitter evolution for all time could have a large effect on the behavior of $\hat{\phi}_\ell^{RMS}$ at large times. It would therefore be important to calculate this behavior under more realistic assumptions, but we have not yet done so.

Note also that for the special case of $\eta = 0$ (or equivalently, $\mu = 0$), Eqs. (6.9-10) indicate that $<\hat{\phi}_\ell^2>$ approaches a constant at large times. On the other hand, a major point is made in Refs. [15] and [16] of the fact that $<\phi^2>$ grows at large times as $\frac{1}{4\pi^2}\chi^3 t$. The discrepancy is caused by the fact that we are using a fixed coordinate smearing length, while the regularization technique used in Refs. [15] and [16] corresponds to using a fixed short-distance cut-off in physical units. If we were to use a fixed physical smearing length, we would also find that $<\hat{\phi}_\ell^2>$ behaves as $\frac{1}{4\pi^2}\chi^3 t$ at late times.

We can now explore what happens as the parameters are varied. Figure 7 shows the behavior of $\dot{\phi}_\ell^{RMS}$ for various values of η, again using $\lambda = 10^{-12}$. All the curves are drawn for $T_0 \equiv \chi$, and $T_0\ell = 1$. On each curve, A denotes the point at which $\dot{\phi}_\ell^{RMS} = \phi_c$, B denotes $T = T_c$, C denotes $T = T_{decS}$, and D denotes $T = \chi$. The differences between the curves at early times are due entirely to the different values of χ (and hence T_0), which is given by Eq. (6.4).

Figure 8 shows the effect of varying $T_0\ell$. All the curves are drawn for $\eta = 0.2$, $T_0 \equiv \chi$, and $\lambda = 10^{-12}$. The upper three curves are drawn for fixed values of $T_0\ell$, corresponding to smearing over a fixed coordinate wavelength. This type of smearing is relevant when one is interested in following the evolution of an expanding region of space. The lower three curves correspond to fixed values of $T_0\ell e^{\chi t}$, so in this case the physical smearing length is held fixed. The behavior is very different at early times, but for $\mu > 0$ and $\lambda \ll 1$ it is indistinguishable at late times.

Figure 9 shows the effect of varying λ. All the curves are drawn for $\eta = 0.2$ and $T_0 \equiv \chi$. The upper curves show the effect of a fixed coordinate smearing length ($T_0\ell = 1$) and the lower curves show a fixed physical smearing length $T_0\ell e^{\chi t} = 1$.

Finally, we can investigate the range of the parameters λ and η which leads to an acceptable inflationary scenario. One must bear in mind, of course, that our calculation applies to only a narrow range of conceivable particle theories. Most theories would involve a multiplet of scalar fields, and an effective potential which is more complicated due to couplings to other fields. However, it is still reassuring to discover that a single scalar field, coupled to no other fields, can by itself be the driving force of an acceptable inflationary scenario.

To determine an acceptable range of parameters, we must first calculate how much inflation is necessary in this model. The entropy density in the universe today is dominated by the background radiation of photons and neutrinos, and is given roughly by

$$s_0 \simeq 3{,}000 \text{ cm}^{-3} \tag{6.11}$$

in units with Boltzmann's constant k set equal to one. Taking the radius R_0 of the observed

universe today as 10^{10} light-years, we find

$$R_0^3 s_0 \simeq 3 \times 10^{87}. \tag{6.12}$$

Since this quantity is essentially conserved in the post-inflationary era, it must have had this value since the reheating which occurred at the end of inflation. If we assume that the reheating is fast compared to χ^{-1}, then the reheating temperature is determined simply by conservation of energy, $\rho_{th} = \rho_0$, using Eqs. (3.6), (6.5), and (6.1):

$$T_r^4 = \frac{135\lambda}{8\pi^4\eta^2 N_{eff}} M_P^4. \tag{6.13}$$

The entropy density immediately after reheating is given by

$$\begin{aligned} s_r &= \frac{2\pi^2}{45} N_{eff} T_r^3 \\ &= \left[\frac{3}{160\pi^4}\frac{\lambda^3}{\eta^6} N_{eff}\right]^{1/4} M_P^3. \end{aligned} \tag{6.14}$$

Thus, immediately after reheating, the radius R_r of the region which will evolve to become the observed universe is given by

$$R_r^3 s_r = R_0^3 s_0. \tag{6.15}$$

We assume that as inflation begins (at $T \approx T_{decS}$), the regions of homogeneity have typical sizes of order χ^{-1}, the Hubble distance. Inflation must then continue long enough for this length to be stretched to R_r, so the duration Δt of the inflationary era must satisfy

$$e^{\chi \Delta t} \gtrsim \chi R_r, \tag{6.16}$$

which implies

$$\chi\,\Delta t \gtrsim 68 + \frac{1}{4}\ln\lambda - \frac{1}{2}\ln\eta - \frac{1}{12}\ln N_{eff}. \tag{6.17}$$

We must now compare the above expression with the amount of inflation which is expected to occur in this model. Inflation begins roughly when $T = T_{decS}$; using Eqs. (6.6) and (3.14), one finds that this condition is met at time t_i, where

$$\chi t_i \approx -\frac{1}{4}\ln\lambda + \frac{1}{2}\ln\eta + \frac{1}{4}\ln N_{eff} - \ln(M_P/T_0). \tag{6.18}$$

As we will discuss more fully in the next section, we expect inflation to end roughly when $\dot{\phi}_t^{RMS} \approx \phi_c$. Using Eqs. (6.9a), (6.10), (6.2), and (6.4), one sees that this condition is met at time t_f given by

$$\chi t_f \approx -1 - \ln\left(\frac{M_P}{T_0}\right) + \ln\eta + \frac{1}{2p-3}\left\{\ln\eta - \frac{1}{2}\ln\lambda - \ln\left[\frac{\Gamma^3(p)}{\pi^{5/2}(p-1)\Gamma(p+\frac{1}{2})}\right]\right\}. \tag{6.19}$$

So

$$\chi(t_f - t_i) \approx -1 - \frac{1}{4}\ln N_{eff} + \frac{1}{2p-3}\left\{\frac{1}{2}\left(p-\frac{5}{2}\right)\ln\lambda + \left(p-\frac{1}{2}\right)\ln\eta - \ln\left[\frac{\Gamma^3(p)}{\pi^{5/2}(p-\frac{1}{2})\Gamma(p+\frac{1}{2})}\right]\right\} \tag{6.20}$$

Comparing with Eq. (6.17), one finds that sufficient inflation requires

$$\lambda \lesssim \eta^{4(p-1)}\left[\frac{\pi^{5/2}(p-1)\Gamma(p+\frac{1}{2})}{\Gamma^3(p)}\right]^2 N_{eff}^{-(2p-3)/3} e^{-138(2p-3)}. \tag{6.21}$$

The expression on the right-hand-side is rather complicated, so a graph of its value is shown in Figure 10.

VII. Cosmological Density Fluctuations

One of the most fascinating features of the inflationary universe model is the manner in which it accounts for cosmological density fluctuations. While earlier cosmological models relied on the introduction of an ad hoc spectrum of primordial fluctuations, in the inflationary model both the large scale homogeneity and the residual density fluctuations are viewed as consequences of the underlying particle physics. The large scale homogeneity is a direct consequence of the tremendous expansion, and the residual fluctuations are relics of the zero point quantum fluctuations in the early universe. While quantum fluctuations are normally relevant only on microscopic distance scales, the inflationary models have the enticing property that microscopic distance scales in the early universe are stretched to astronomical scales today. In this section we will discuss the origin of these fluctuations in the context of the exactly soluble model described in Section III.

We begin by reviewing the semiclassical approach which has been used in the literature,[5] following most closely the approach used in our own paper.[36] However, we will adapt this approach to a scalar field with the potential energy function used in Section III.

All of the papers in Ref. [5] introduce a homogeneous solution $\phi_0(t)$ to the classical equations of motion:

$$\ddot{\phi}_0 + 3\chi\dot{\phi}_0 = -\frac{\partial V}{\partial\phi}. \tag{7.1}$$

The full scalar field is then decomposed into a classical and quantum part, according to

$$\phi(\vec{x},t) = \phi_0(t) + \delta\phi(\vec{x},t), \tag{7.2}$$

Assuming that $|\delta\phi| \ll \phi_0$, $\delta\phi(\vec{x},t)$ is then treated as a free quantum field obeying the linearized equation

$$\delta\ddot{\phi} + 3\chi\,\delta\dot{\phi} - e^{-2\chi t}\vec{\nabla}^2\,\delta\phi = -\frac{\partial^2 V}{\partial\phi^2}(\phi_0)\,\delta\phi. \tag{7.3}$$

As we mentioned in the introduction, the precise meaning of $\phi_0(t)$ in the quantum mechanical context is never properly stated in these papers.

Applying this approach to the model described in Section III, one has

$$\frac{\partial V}{\partial\phi} = -\mu^2\phi + \lambda\phi^3. \tag{7.4}$$

For early times when $\phi \ll \phi_c = \mu/\sqrt{\lambda}$, one can neglect the $\lambda\phi^3$ term in the equations of motion, so that

$$\ddot{\phi}_0 + 3\chi\dot{\phi}_0 = \mu^2\phi_0, \tag{7.5a}$$

$$\delta\ddot{\phi} + 3\chi\,\delta\dot{\phi} = \mu^2\,\delta\phi + e^{-2\chi t}\vec{\nabla}^2\,\delta\phi. \tag{7.5b}$$

If λ is sufficiently small, it was shown in the last section that there is a long time interval ($\chi\Delta t \gtrsim 70$) for which the above equations apply, so it makes sense to look at the large time behavior of the solutions. We will call this time period the "middle rollover period"—the period which is early enough so that $\phi_0 \ll \phi_c$, but late enough so that the solutions

to Eqs. (7.5) are well approximated by their asymptotic forms. The general solution to (7.5a) involves a growing and a decaying exponential, and the large time behavior is given by the growing mode

$$\phi_0(t) \simeq \phi_a e^{\frac{1}{3}(2p-3)\chi t}, \tag{7.6}$$

where ϕ_a is a constant, and p is given by Eq. (3.20). For large times one can neglect the spatial gradient in (7.3), so the large time behavior is given by

$$\delta\phi(\vec{x},t) \simeq f(\vec{x}) e^{\frac{1}{3}(2p-3)\chi t}, \tag{7.7}$$

for some function $f(\vec{x})$.

One can then define the quantity $\delta r(\vec{x})$ by[37]

$$\delta r(\vec{x}) = -\lim_{t\to\infty} \frac{\delta\phi(\vec{x},t)}{\dot{\phi}_0(t)}. \tag{7.8}$$

This quantity is interpreted as an asymptotic time delay, since at large times one can write

$$\begin{aligned} \phi(\vec{x},t) &= \phi_0(t) + \delta\phi(\vec{x},t) \\ &\simeq \phi_0(t) - \dot{\phi}_0(t)\,\delta r(\vec{x}) \\ &\simeq \phi_0[t - \delta r(\vec{x})]. \end{aligned} \tag{7.9}$$

To continue, one Fourier expands the spatially inhomogeneous functions $\delta r(\vec{x})$ and $\delta\phi(\vec{x},t)$, using the standard notation

$$f(\vec{x}) = \int d^3k\, e^{i\vec{k}\cdot\vec{x}} \tilde{f}(\vec{k}). \tag{7.10}$$

One can then show that the density fluctuations are determined (in lowest order perturbation theory) by $\delta\tilde{r}(\vec{k})$. To quantify the density perturbations, recall that they result in oscillations with a time-independent amplitude once the wavelength becomes much less than the Hubble length (assuming that this occurs during the radiation-dominated era). They can then be characterized by the root-mean-square value (averaged over time) of these oscillations, and it can be shown[38] that

$$\frac{\delta\tilde{\rho}_{\rm rms}(\vec{k})}{\rho} = 2\sqrt{2}\chi\,\delta\tilde{r}(\vec{k}). \tag{7.11}$$

The only remaining problem is to determine $\delta\phi(\vec{x},t)$, which is of course a stochastic quantity. We describe the root-mean-square fluctuations of any (translationally invariant) stochastic function $f(\vec{x})$ by the quantity

$$\Delta f(\vec{k}) \equiv \left\{ \frac{k^3}{(2\pi)^3} \int d^3x\, e^{i\vec{k}\cdot\vec{x}} < f(\vec{x}) f(\vec{0}) > \right\}^{1/2}, \tag{7.12}$$

where $< >$ denotes the usual expectation value. To determine $\Delta\phi(\vec{x},t)$, one treats $\delta\phi(\vec{x},t)$ as a free quantum field in de Sitter space. Following the approach of Ref. [36] (which is quite similar in this respect to the other references), one begins by rewriting Eq. (7.5b) for $\delta\tilde{\phi}(\vec{k},t)$, obtaining

$$\delta\ddot{\tilde{\phi}} + 3\chi\,\delta\dot{\tilde{\phi}} = \mu^2\,\delta\tilde{\phi} - e^{-2\chi t}k^2\,\delta\tilde{\phi}. \tag{7.13}$$

There is then a time

$$t^*(k) = \chi^{-1}\ln(k/\mu) \tag{7.14}$$

at which the two terms on the right-hand-side of the equation are equal. For $t \ll t^*(k)$, the mass term is negligible and the field is well-approximated by a free massless (minimally coupled) scalar field in de Sitter space. The two-point function is then well-known,[32,31,38] and is given by Eq. (3.37) in the limit $T_0 \to 0$. One then has

$$\Delta\phi(\vec{x},t) \simeq \left\{ \frac{1}{16\pi^3}\left[\chi^2 + k^2 e^{-2\chi t}\right] \right\}^{1/2}. \tag{7.15}$$

On the other hand, for $t \gg t^*(k)$ one can write

$$\Delta r(\vec{k}) \simeq \frac{\Delta\phi(\vec{k},t)}{\dot{\phi}_0(t)}. \tag{7.16}$$

If one assumes that both of these approximations are reasonably accurate at $t = t^*(k)$, then one can match them at that time to determine[39] $\Delta r(\vec{k})$. Using Eqs. (7.11), (7.14-16), and (7.6), one has the final result

$$\frac{\Delta\rho_{\rm rms}(\vec{k})}{\rho} \simeq \frac{\sqrt{2(1+\eta)}}{\pi^{3/2}(2p-3)}\left(\frac{\chi}{\phi_a}\right)\left(\frac{\mu}{k}\right)^{\frac{1}{3}(2p-3)}. \tag{7.17}$$

It should be noted that the above description relied on the assumption that the $\lambda\phi^3$ term in the equation of motion could be neglected at time $t^*(k)$, an assumption which is valid

provided that

$$\left(\frac{k}{\mu}\right)^{2p-3} \ll \frac{\phi_c^2}{\phi_a^2}. \tag{7.18}$$

The above method seems reasonably convincing, and its consequences (in the context of the Coleman-Weinberg potential) have been accepted by a number of authors.[5] However, it clearly has at least two deficiencies. First, there is the second question which we discussed in the introduction: the classical solution $\phi_0(t)$ has no clear interpretation in the quantum-mechanical context. In particular, it is clearly **not** the expectation value of the quantum operator. Second, the matching condition used to determine the final answer is clearly only an approximation. We will now discuss how both of these deficiencies can be overcome by using the exactly soluble model of Section III.

To understand the decomposition (7.2), one must remember that the goal of the inflationary scenario is to cause some very small region of pre-inflationary space to evolve into a region comparable to the observed universe. Let the coordinate radius of this region be denoted by a, and then choose some $\kappa \ll 1/a$. One can then consider a Fourier expansion of the smeared field $\hat{\phi}_\ell(\vec{x},t)$, as given by Eq. (5.2). One must choose ℓ small enough so that the fluctuations on the length scales of interest will be visible, yet not so small that fluctuations on irrelevantly small scales become dominant. Now let ϕ_0 denote the sum of all terms in the Fourier expansion with $|\vec{k}| > \kappa$. With this definition ϕ_0 is not really independent of $\vec{x}$, but its $\vec{x}$-dependence can be ignored because ϕ_0 is essentially uniform over the observed universe.

According to the discussion of Section IV, each mode of the scalar field can be considered classical when its "effective wavelength" $2\pi e^{Xt}/\sqrt{k^2 + \frac{1}{4}\lambda T_0^2}$ is long compared to the Hubble length. Once this condition holds for the wave number κ, $\phi_0(t)$ can be regarded as a classical variable evolving according to the classical equations of motion. These classical trajectories can be parameterized at large times by a single parameter, the constant ϕ_a of Eq. (7.6). The precise value of ϕ_a is not predictable, but instead ϕ_a is described by a classical probability distribution. In this case the distribution is Gaussian with a mean of zero, but nonetheless any given observer (except for a set of measure zero) will measure a nonzero value for ϕ_a. Note that the value of ϕ_a determines how much

inflation the region will undergo before the inflationary era is ended by reheating. For the model to be plausible, one must check that there is a high probability that ϕ_a is small enough to allow for sufficient inflation.

Note that the decomposition (7.2) will make sense only if $|\delta\phi| \ll \phi_0$, and this requirement will prevent one from choosing κ or ℓ too small. However, there is a wide latitude in the choice of these parameters.

The asymptotic behavior of $\dot{\phi}_\ell^{RMS} \equiv < \dot{\phi}_\ell^2 >^{1/2}$ was discussed in Section VI (with details in Appendix D), and it was found to be dominated by wavelengths of order $1/\sqrt{\lambda}$ times the thermal wavelength T^{-1}. Thus, as long as one chooses $\kappa > \sqrt{\lambda}T_0$ and ℓ of order T_0^{-1}, for large times one has

$$< \dot{\phi}_\ell^2 > \simeq < \phi_a^2 > e^{(2p-3)t} \simeq < \phi_0(t)^2 > . \tag{7.19}$$

Thus, the criterion for sufficient inflation adopted in Section VI is completely consistent with our interpretation of $\phi_0(t)$.

Note that Eq. (7.19) is actually valid for a very wide range of choices for the smearing parameter ℓ. One must of course choose $\ell < 1/(\sqrt{\lambda}T_0)$, so that the dominant wavelengths are not suppressed by the smearing process. And one must choose ℓ large enough so that the residual small-scale quantum fluctuations, which make a contribution to $< \dot{\phi}_\ell^2 >$ of order $\ell_{\rm phys}^{-2} = e^{-2Xt}\ell^{-2}$, do not rival the leading term.

We can now complete the calculation. Since the behavior of the quantum field $\phi(\vec{x},t)$ for all time was completely determined in Section III, there is no need for us to use an approximate matching condition as in the derivation of Eq. (7.17). The exact equal-time propagator was given as Eq. (3.36), from which it follows that

$$\Delta\phi(\vec{k},t) = \left\{\frac{k^3}{(2\pi)^3}|\psi(\vec{k},t)|^2 \coth\left(\tfrac{1}{2}\Theta_{\vec{k}}\right)\right\}^{1/2}, \tag{7.20}$$

where $\psi(\vec{k},t)$ and $\Theta_{\vec{k}}$ are defined by Eqs. (3.28) and (3.32b). The asymptotic behavior at large times can be found by using Eqs. (C.3), yielding

$$\Delta\phi(\vec{k},t) \sim \frac{2^p\Gamma(p)}{2^{5/2}\pi^2}\frac{k^{3/2}}{\chi^{1/2}}\left(\frac{\chi}{\sqrt{k^2+\gamma^2}}\right)^p \coth^{1/2}\left(\tfrac{1}{2}\Theta_{\vec{k}}\right) e^{\frac{1}{2}(2p-3)Xt}. \tag{7.21}$$

Using (7.21) to calculate the density fluctuations, one finds

$$\frac{\Delta\rho_{\rm rms}(\vec{k})}{\rho} = \frac{2^p\Gamma(p)}{(2p-3)\pi^2}\frac{k^{3/2}}{\phi_a\chi^{1/2}}\left(\frac{\chi}{\sqrt{k^2+\tilde{\gamma}^2}}\right)^p \coth^{1/2}(\tfrac{1}{2}\Theta_k). \tag{7.22}$$

All of the visible structure in the universe would come from wavelengths much shorter than thermal ($k \gg T_0$), in which case the formula above reduces to

$$\frac{\Delta\rho_{\rm rms}(\vec{k})}{\rho} = \frac{2^p\Gamma(p)}{(2p-3)\pi^2}\left(\frac{\chi}{\phi_a}\right)\left(\frac{\chi}{k}\right)^{\frac{1}{2}(2p-3)}. \tag{7.23}$$

In the context of our assumptions, this answer is exact.

Note that both expressions (7.17) and (7.23) diverge as $\eta \to 0$, because in this limit $p \to 3/2$. This divergence, however, is not physical; in this limit $\mu \to 0$, and so the inequality (7.18) will be violated for all k.

Note also that both formulas (7.17) and (7.23) imply that $\Delta\rho/\rho \propto k^{-\frac{1}{2}(2p-3)}$. This is a very weak power dependence, which becomes completely flat as $\eta \to 0$. For $\eta = 0.2$, for example, the power dependence is $k^{-.065}$.

The ratio of the exact answer (7.23) to the approximate answer (7.17) depends only on η, and is plotted in Figure 11. Considering that the expression (7.17) was intended as only an order of magnitude estimate, the agreement is amazingly good.

Eq. (7.23) for $\Delta\rho/\rho$ shows that the quantity is inversely proportional to ϕ_a, so one might infer that the degree of inhomogeneity of the resulting model universe is determined by the value which this random variable happens to take. This inference, however, would be incorrect. The complication is that $\Delta\rho/\rho$ is expressed as a function of the wave number k, which must be related to physical length scales before the formula can be interpreted.

The wave number k arises from a Fourier transform with respect to the coordinate x, which is normalised so that the scale factor in the de Sitter phase has the simple form $e^{\chi t}$, as in Eq. (3.1). The correspondence between this length scale and the length scale of the present universe will be strongly dependent on how much inflation occurs, which depends on the value of ϕ_a.

To see how this works quantitatively, note that Eq. (7.6) can be rewritten as

$$\phi_0(t') \simeq \phi_c e^{\frac{1}{2}(2p-3)\chi t'}, \tag{7.24}$$

where

$$t' = t + \frac{2}{(2p-3)\chi}\ln(\phi_a/\phi_c). \tag{7.25}$$

Note that Eq. (7.24) involves no random variables, and can serve as a starting point for calculating the subsequent evolution of the universe as a function of t'. All of the stochasticity has been relegated to Eq. (7.25), which relates the time variable t, which we used to describe the inflationary era, to the time variable t' which will be used to describe all the the post-inflationary evolution.

In order to have a definite coordinate length scale in the post-inflationary era, we can switch to a new coordinate system $(\vec{x}', t')$ during the middle rollover period. The metric for the $(\vec{x}, t)$ coordinate system is described by the de Sitter expression (3.1), so one can write

$$\begin{aligned} ds^2 &= -dt^2 + e^{2\chi t}d\vec{x}^2 \\ &= -dt'^2 + e^{2\chi t'}d\vec{x}'^2, \end{aligned} \tag{7.26}$$

provided that one defines

$$\vec{x}' = \exp\left\{\frac{2}{2p-3}\ln(\phi_c/\phi_a)\right\}\vec{x}. \tag{7.27}$$

One then has

$$\vec{k}' = \exp\left\{-\frac{2}{2p-3}\ln(\phi_c/\phi_a)\right\}\vec{k}, \tag{7.28}$$

and Eq. (7.23) can then be rewritten as

$$\frac{\Delta\rho_{\rm rms}(\vec{k}')}{\rho} = \frac{2^p\Gamma(p)}{(2p-3)\pi^2}\left(\frac{\chi}{\phi_a}\right)\left(\frac{\chi}{k'}\right)^{\frac{1}{2}(2p-3)}. \tag{7.29}$$

Thus, when expressed in terms of variables which have definite meaning in the post-inflationary era, $\Delta\rho/\rho$ does not depend on any random variables.

VIII. Conclusion

The purpose of this paper has been an attempt to improve our understanding of the slow-rollover phase transition which characterizes inflationary models. Specifically, we have constructed an approximate but exactly soluble model for the behavior of the scalar field during such a phase transition. We believe that this exactly soluble model can serve

as the zero order approximation in a perturbative calculation of a realistic model, but we have not yet attempted such a calculation.

The exactly soluble model is based on three simplifying assumptions. First, we assumed an exactly de Sitter metric for all time. Second, we assumed that the scalar field could be treated by a free quantum field theory, with a time-dependent potential function $V(\phi) = -\frac{1}{2}(\mu^2 - \frac{1}{4}\lambda T^2)\phi^2$, where the background temperature T behaves as $T_0 e^{-\chi t}$. Finally, we assumed that the initial state could be specified at asymptotically early times by describing each mode variable by a thermal equilibrium ensemble.

We have studied a number of consequences of this exactly soluble model. The formalism developed in this paper allows one to calculate the expectation value of an arbitrary function of $\phi(\vec{x}, t)$. We have also studied the behavior of the system at large times, and have concluded that it can be described by a probability distribution of classical trajectories. In order to discuss quantities which are in principle measurable, we have made use of the smeared field $\hat{\phi}_\ell$, where ℓ denotes the smearing length. The probability distribution for this quantity was calculated, and numerical data for the expectation value of its square was presented. In this model one can calculate how much inflation is expected to occur, and we derived an inequality which shows the range of parameters which lead to sufficient inflation.

Finally we examined the question of density fluctuations. We showed how to decompose the quantum operator $\phi(\vec{x}, t)$ into a piece $\phi_0(t)$ which is effectively homogeneous, and a piece $\delta\phi(\vec{x}, t)$ which describes the spatial inhomogeneities. We calculated the root-mean-square inhomogeneities in $\delta\phi(\vec{x}, t)$, and then showed how to infer the root-mean-square density fluctuations $\Delta\rho/\rho$.

For all the questions that we have studied so far, we have found that the more naive approaches which had been used earlier were essentially correct.

A number of topics remain open for future research. For example, the assumption of exact de Sitter evolution is certainly invalid at early times, and it would be interesting to determine the effect of an initial Friedmann-Robertson-Walker phase. In addition, there is no real justification for our assumption of a thermally distributed initial state, so it

would be useful to explore other possibilities. Finally, it would be very worthwhile to attempt a perturbative calculation in a realistic model, using the exactly soluble model as a starting point. It may not be tractable to obtain reliable numerical results, but it would be worthwhile simply to show as a matter of principle that that one could compute corrections, and that they are small in the case of weak coupling.

Acknowledgements

We would like to acknowledge discussions with a number of other physicists, including Bill Bardeen, Jim Bardeen, Stephen Hawking, Chris Hill, Jim Peebles, and Bob Wald. These discussions not only provided some useful insights, but the skepticism voiced by some of these people forced us to attempt to sharpen our arguments.

Both authors would like to acknowledge the hospitality of the Aspen Center for Physics, where part of this work was carried out. A.H.G. was supported in part through funds provided by the U.S. Department of Energy (DOE) under contract DE-AC02-76ERO3069, in part by the National Aeronautics and Space Administration (NASA) under grant NAGW-553, and in part by an Alfred P. Sloan Fellowship. S.-Y. P. was supported in part through funds provided by the Department of Energy under the Outstanding Junior Investigator Program.

Appendix A. Relationship to the Standard Notation

Since the notation used in Section III was both unfamiliar and a little awkward, it is useful to translate the results into the standard expansion in terms of complex exponentials.

Eq. (3.15) can be replaced by the simpler expansion

$$\phi(\vec{x},t)=\frac{1}{(2\pi)^{3/2}}\left(\frac{2\pi}{b}\right)^{3/2}\sum_{\substack{\vec{k}=(\frac{2\pi}{b})\vec{n}\\ \vec{n}\ \text{integer}}}\left[c(\vec{k})e^{i\vec{k}\cdot\vec{x}}\psi(\vec{k},t)+c^{\dagger}(\vec{k})e^{-i\vec{k}\cdot\vec{x}}\psi^{*}(\vec{k},t)\right], \tag{A.1}$$

where $\psi(\vec{k},t)$ is again given by Eq. (3.28). The running wave annihilation operators $c(\vec{k})$ can be related to the standing wave annihilation operators $a_{\pm}(\vec{k})$ by the equations

$$\begin{aligned} c(\vec{k})&=\frac{a_{+}(\vec{k})-ia_{-}(\vec{k})}{\sqrt{2}} \qquad \text{if } \vec{k}\neq 0,\\ c(\vec{0})&=a(\vec{0}), \end{aligned} \tag{A.2}$$

which for $\vec{k}\neq 0$ can be inverted to give

$$\begin{aligned} a_{+}(\vec{k})&=\frac{1}{\sqrt{2}}[c(\vec{k})+c(-\vec{k})],\\ a_{-}(\vec{k})&=\frac{i}{\sqrt{2}}[c(\vec{k})-c(-\vec{k})]. \end{aligned} \tag{A.3}$$

One can easily check that the operators $c(\vec{k})$ obey the commutation relations

$$[c(\vec{k}),c^{\dagger}(\vec{k}')]=\delta_{\vec{k},\vec{k}'}. \tag{A.4}$$

To take the continuum limit, one must rescale the annihilation operators by

$$d(\vec{k})\equiv\left(\frac{b}{2\pi}\right)^{3/2}c(\vec{k}), \tag{A.5}$$

so that the new annihilation operators satisfy the commutation relations

$$[d(\vec{k}),d^{\dagger}(\vec{k}')]=\delta^{3}(\vec{k}'-\vec{k}). \tag{A.6}$$

The expansion for $\phi(\vec{x},t)$ is then given by the following simple expression[40]:

$$\phi(\vec{x},t)=\frac{1}{(2\pi)^{3/2}}\int d^{3}\vec{k}\left\{d(\vec{k})e^{i\vec{k}\cdot\vec{x}}\psi(\vec{k},t)+d^{\dagger}(\vec{k})e^{-i\vec{k}\cdot\vec{x}}\psi^{*}(\vec{k},t)\right\}. \tag{A.7}$$

The expressions for the expectation values can also be translated in a simple way. From Eqs. (A.2) and (3.32), one has

$$<c^{\dagger}(\vec{k}')c(\vec{k})>=\frac{1}{e^{\Theta_{\vec{k}}}-1}\delta_{\vec{k}',\vec{k}}, \tag{A.8a}$$

and of course

$$<c(\vec{k}')c(\vec{k})>=<c^{\dagger}(\vec{k}')c^{\dagger}(\vec{k})>=0. \tag{A.8b}$$

The expectation values for the continuum normalized creation and annihilation operators are then given by

$$\begin{aligned} <d^{\dagger}(\vec{k}')d(\vec{k})>&=\frac{1}{e^{\Theta_{\vec{k}}}-1}\delta^{3}(\vec{k}'-\vec{k})\\ <d(\vec{k}')d(\vec{k})>&=<d^{\dagger}(\vec{k}')d^{\dagger}(\vec{k})>=0. \end{aligned} \tag{A.9}$$

Appendix B. Functional Schrödinger Picture for Field Theory

For our field theory problem a description similar to the upside-down harmonic oscillator can be given using the functional Schrödinger picture for field theory. This is an unfamiliar method for probing field theory, but brings new insights to our subject: it enables us to obtain the time dependent wave function and, therefore, gives a clear description for the time evolution of the system as in the case of quantum mechanics.

1. "Ground State" Wave Functional

In the functional Schrödinger picture an abstract quantum mechanical state $|\psi>$ is realized by $\Psi(\phi,t)$ which is a wave functional of the c-number function $\phi(\vec{x})$ at a fixed time. The action of the operator $\phi(\vec{x})$ on $|\psi>$ is realized by multiplying $\Psi(\phi,t)$ by $\phi(\vec{x})$, and the action of the canonical momentum $\pi(\vec{x})$ is realized by functional differentiation:

$$\phi(\vec{x})|\psi> \rightarrow \phi(\vec{x})\Psi(\phi,t) \tag{B.1a}$$

$$\pi(\vec{x})|\psi> \rightarrow \frac{\hbar}{i}\frac{\delta}{\delta\phi(\vec{x})}\Psi(\phi,t). \tag{B.1b}$$

Then, the functional Schrödinger equation for our idealized model is

$$i\hbar\frac{\partial}{\partial t}\Psi = \frac{1}{2}\int d^3x\left\{-e^{-3\chi t}\hbar^2\frac{\delta^2}{\delta\phi^2} + e^{\chi t}\left[(\vec{\nabla}\phi)^2+\gamma^2\phi^2\right] - e^{3\chi t}\mu^2\phi^2\right\}\Psi. \tag{B.2}$$

Since it is a free theory, in momentum space the mode variables $\sigma(\vec{0})$ and $\sigma_{\pm}(\vec{k})$, defined in Eq. (3.15), completely decouple from each other and the Hamiltonian is given by Eq. (3.23):

$$H = \sum_{\alpha} H_{\alpha}(\sigma_{\alpha},\pi_{\alpha}), \tag{B.3}$$

where σ_{α} denotes the mode variables and the sum $\sum_{\alpha}$ means the sum over $\sigma(\vec{0})$, $\sigma_{+}(\vec{k})$ and $\sigma_{-}(\vec{k})$, with each pair $(\vec{k},-\vec{k})$ counted only once, as in the text. The wave functional of any energy eigenstate can then be factorized:

$$\Psi = \prod_{\alpha}\Psi_{\alpha}(\sigma_{\alpha},t), \tag{B.4}$$

where Ψ_{α} denotes the wave function for each σ_{α} and satisfies the Schrödinger equation

$$\begin{aligned} i\hbar\frac{\partial\Psi_{\alpha}}{\partial t} &= H_{\alpha}\Psi_{\alpha} \\ &= \left\{-\frac{1}{4}\left(\frac{b}{2\pi}\right)^3\hbar^2 e^{-3\chi t}\frac{\partial^2}{\partial\sigma_{\alpha}^2}\right. \\ &\quad \left. + e^{3\chi t}\left(\frac{2\pi}{b}\right)^3\left[e^{-2\chi t}(\vec{k}_{\alpha}^{\,2}+\gamma^2)-\mu^2\right]\sigma_{\alpha}^2\right\}\Psi_{\alpha} \end{aligned} \tag{B.5}$$

Note that the above equation describes a system which behaves at very early times as a simple harmonic oscillator with frequency $\omega_{\alpha}(t) = \sqrt{\vec{k}_{\alpha}^{\,2}+\gamma^2 e^{-\chi t}}$. Our first goal is to find the "ground state" wave functional for each σ_{α}, where by "ground state" we mean the state which behaves as a harmonic oscillator ground state in the asymptotic past:

$$\Psi_{\alpha}^{0} \xrightarrow[t\rightarrow-\infty]{} \exp\left\{-2\left(\frac{2\pi}{b}\right)^3 e^{3\chi t}\frac{1}{2\hbar}\omega_{\alpha}(t)\sigma_{\alpha}^2\right\}. \tag{B.6}$$

It is straightforward to show that Eq. (B.5) has an exact solution with a Gaussian form

$$\Psi_{\alpha}(\sigma_{\alpha},t) = A(\vec{k}_{\alpha},t)\exp\left\{-2\left(\frac{2\pi}{b}\right)^3 B(\vec{k}_{\alpha},t)\sigma_{\alpha}^2\right\}, \tag{B.7a}$$

where

$$B(\vec{k},t) = -\frac{i}{2\hbar}e^{3\chi t}\frac{\partial}{\partial t}\ln\varphi^*(\vec{k},t) \tag{B.7b}$$

and $\varphi(\vec{k},t)$ is any solution to the equation of motion (3.18). (We have expressed $B(\vec{k},t)$ in terms of φ^* rather than φ in order to simplify the form of subsequent results.) The most general solution to (3.18) can be written as

$$\varphi(\vec{k},t) = \frac{1}{2}\sqrt{\frac{\pi\hbar}{\chi}}e^{-\frac{3}{2}\chi t}\left[c_1(\vec{k})H_p^{(1)}(z)+c_2(\vec{k})H_p^{(2)}(z)\right], \tag{B.7c}$$

where z is given by Eq. (3.21). Here $c_1(\vec{k})$ and $c_2(\vec{k})$ are arbitrary complex functions. Since $B(\vec{k},t)$ is unchanged when $\varphi(\vec{k},t)$ is multiplied by a time-independent function of $\vec{k}$, it is possible to fix the normalization of φ by requiring

$$|c_1(\vec{k})|^2 - |c_2(\vec{k})|^2 = 1. \tag{B.8}$$

Note that $\varphi(\vec{k},t)$ is simply a Bogoliubov transformation of the mode function $\psi(\vec{k},t)$ of Eq. (3.28), which was used in the expansion of $\phi(\vec{x},t)$ in creation and annihilation operators.[41]

Using the normalization convention (B.8), the mode function $\varphi(\vec{k},t)$ can be shown to obey a normalization condition identical to (3.29). This normalization condition allows one to write $B(\vec{k},t)$ explicitly in terms of its real and imaginary parts:

$$B(\vec{k},t)=\frac{1}{4|\varphi|^2}\left[1-\frac{i}{\mathcal{K}}e^{3\chi t}\frac{\partial}{\partial t}|\varphi|^2\right]. \tag{B.9}$$

The magnitude of $A(\vec{k},t)$ can be determined by the normalization of $\Psi_\alpha(\sigma_\alpha,t)$, which gives

$$|A(\vec{k},t)|=\left\{\left(\frac{b}{2\pi}\right)^3\pi|\varphi(\vec{k},t)|^2\right\}^{-1/4}. \tag{B.10}$$

The determination of the functions $c_1(\vec{k})$ and $c_2(\vec{k})$ is dictated by the asymptotic behavior (B.6), which implies that

$$B(\vec{k},t)\xrightarrow[t\to-\infty]{}\frac{1}{2\mathcal{K}}\sqrt{\vec{k}^2+\gamma^2}e^{2\chi t}, \tag{B.11}$$

Using the asymptotic behavior of the Hankel functions given in Eq. (C.2), one finds that (B.11) is satisfied for

$$c_1\equiv 1,\qquad c_2\equiv 0, \tag{B.12}$$

which agrees exactly with the mode function $\psi(\vec{k},t)$ used in Section III. From Eqs. (B.7a) and (B.9) we have immediately that

$$<\sigma_\alpha^2>=\frac{1}{8\left(\frac{2\pi}{b}\right)^3\mathrm{Re}\,B}=\frac{1}{2}\left(\frac{b}{2\pi}\right)^3|\psi|^2, \tag{B.13}$$

which is exactly the same as the expression in Eq. (3.34) except for the factor $\coth\left(\frac{1}{2}\Theta_\alpha\right)$ which comes from the thermal ensemble average.

2. Classical Behavior at Late Times.

In the functional Schrödinger picture we can explicitly show that the classical description emerges at large times as in the one dimensional quantum mechanical example in

Section II. The behavior of Ψ_α for large t is given by, for $\mu^2>0$,

$$\Psi_\alpha\xrightarrow[t\to\infty]{}\exp\left\{-2\left(\frac{2\pi}{b}\right)^3e^{3\chi t}\left[\frac{\pi\chi}{\mathcal{K}\Gamma^2(p)}\left(\frac{\vec{k}_\alpha^2+\gamma^2}{4\chi^2}e^{-2\chi t}\right)^p-\frac{i}{4\mathcal{K}}(2p-3)\chi\right]\sigma_\alpha^2\right\}. \tag{B.14}$$

Let us observe that operating with the momentum operator on Ψ_α at large times yields

$$\frac{\mathcal{K}}{i}\frac{\partial\Psi_\alpha}{\partial\sigma_\alpha}=(2p-3)\chi\left(\frac{2\pi}{b}\right)^3e^{3\chi t}\sigma_\alpha\Psi_\alpha\{1+\mathrm{O}(z^2)\}, \tag{B.15}$$

where the $\mathrm{O}(z^2)$ correction arises from the nonleading terms in Eq. (C.3).

The $1+\mathrm{O}(z^2)$ on the right-hand side of Eq. (B.15) approaches one for $z\ll 1$ (large t), when the effective wavelength becomes much larger than the horizon length. The first factor is precisely the classical value of $\pi_\alpha(t)=2(2\pi/b)^3e^{3\chi t}\dot{\sigma}_\alpha$ with $\dot{\sigma}_\alpha=\frac{1}{2}(2p-3)\chi\sigma_\alpha$, which is the solution of the classical equation of motion Eq. (3.18) at large times.

The special case of $\mu^2=0$ ($p=\frac{3}{2}$) must be treated separately. From the expression for $H^{(1)}_{3/2}(z)$ in Eq. (C.5), the large t behavior of Ψ_α for $\mu^2=0$ is

$$\Psi_\alpha\xrightarrow[t\to\infty]{}\exp\left\{-2\left(\frac{2\pi}{b}\right)^3\frac{1}{2\mathcal{K}}\left[\frac{(\vec{k}_\alpha^2+\gamma^2)^{3/2}}{\chi^2}+i\frac{\vec{k}_\alpha^2+\gamma^2}{\chi}e^{\chi t}\right]\sigma_\alpha^2\right\}, \tag{B.16}$$

and applying the momentum operator on Ψ_α gives

$$\frac{\mathcal{K}}{i}\frac{\partial\Psi_\alpha}{\partial\sigma_\alpha}=\left[-2\left(\frac{2\pi}{b}\right)^3\frac{\vec{k}_\alpha^2+\gamma^2}{\chi}e^{\chi t}\sigma_\alpha\right]\Psi_\alpha\{1+\mathrm{O}(z)\}. \tag{B.17}$$

The first factor on the right-hand side of Eq. (B.17) is precisely the classical value of π_α for $\mu^2=0$ in the large t limit, and the correction factor at the right approaches one for small z (large t), but not as quickly as in the case of $\mu^2>0$.

Thus, our idealized field theory model is described by classical physics at large times. However, as in the case of the upside-down harmonic oscillator discussed in Section II, it is described not by a single classical trajectory, but by a classical probability distribution

$$f(\pi_\alpha,\sigma_\alpha,t)=|\Psi(\sigma_\alpha,t)|^2\,\delta(\pi_\alpha-(\cdots)), \tag{B.18}$$

where $(\cdots)$ is the classical value of π_α in the large t limit, as shown in Eqs. (B.15) or (B.17). Therefore, the wave functional describes σ_α evolving in the potential according to the classical equation of motion.

3. Probability Distribution at Finite Temperature

So far we have neglected the effects of the thermal ensemble. Since each $\sigma_\alpha(t)$ behaves as a simple harmonic oscillator in thermal equilibrium at early times, one would expect a distribution of excitations for each mode given by $e^{-n\omega_\alpha/T}/\sum_{n=0}^{\infty} e^{-n\omega_\alpha/T}$. Therefore, the probability distribution for σ_α at finite temperature is given by

$$p[\sigma_\alpha, t] \propto \sum_{n=0}^{\infty} e^{-n\Theta_\alpha} |\Psi_\alpha^n(\sigma_\alpha, t)|^2, \tag{B.19}$$

where Θ_α is defined in Eq. (3.32b) and Ψ_α^n is the wave function of the n'th excited state for the mode σ_α, given by

$$\Psi_\alpha^n(\sigma_\alpha, t) = \frac{1}{2^{n/2}} \frac{1}{\sqrt{n!}} e^{in\theta_p(z)} H_n\Big(\sqrt{4(2\pi/b)^3 \,\mathrm{Re}\, B(\vec{k}_\alpha, t)}\,\sigma_\alpha\Big) \Psi_\alpha^0(\sigma_\alpha, t). \tag{B.20}$$

Here the H_n denote the Hermite polynomials, and $\theta_p(z)$ is a phase defined by

$$H_p^{(1)}(z) \equiv M_p(z)\, e^{i\theta_p(z)}. \tag{B.21}$$

Note that $\Psi_\alpha^n(\sigma_\alpha, t)$ looks exactly like the corresponding formula for the ordinary harmonic oscillator, except that the phase factor $e^{in\theta_p(z)}$ replaces the harmonic oscillator phase $e^{-in\omega t}$. The probability distribution can be obtained by the standard harmonic oscillator technique,[34] and we obtain

$$\begin{aligned} p[\sigma_\alpha, t] = &\sqrt{\frac{4}{\pi}\Big(\frac{2\pi}{b}\Big)^3 \,\mathrm{Re}\, B(\vec{k}_\alpha, t) \tanh\frac{1}{2}\Theta_\alpha} \\ &\times \exp\left\{-4\Big(\frac{2\pi}{b}\Big)^3 \,\mathrm{Re}\, B(\vec{k}_\alpha, t) \tanh\Big(\frac{1}{2}\Theta_\alpha\Big)\sigma_\alpha^2\right\}. \end{aligned} \tag{B.22}$$

The mode variables σ_α are Gaussian distributed, with $< \sigma_\alpha^2(t) >$ given by Eq. (3.34).

Appendix C. Useful Properties of Bessel Functions

In this appendix we summarize some useful properties of Bessel functions, as can be found in Refs. [42] or [43]. Following the notation of Ref. [42], Bessel functions of the first kind are denoted by $J_p(z)$, Bessel functions of the second kind (also called Neumann functions) are denoted by $N_p(z)$, and Bessel functions of the third kind (also called Hankel functions) are denoted by $H_p^{(1)}(z)$ and $H_p^{(2)}(z)$.

The Hankel functions are related to $J_p(z)$ and $N_p(z)$ by

$$\begin{aligned} H_p^{(1)}(z) &\equiv J_p(z) + iN_p(z) \\ H_p^{(2)}(z) &\equiv J_p(z) - iN_p(z). \end{aligned} \tag{C.1}$$

The behavior of the Hankel functions for asymptotically large z is given by

$$H_p^{(k)}(z) \sim \sqrt{\frac{2}{\pi z}}\, e^{\pm i\left(z - \frac{1}{2}p - \frac{\pi}{4}\right)} \left\{1 + O\Big(\frac{1}{|z|}\Big)\right\}, \tag{C.2}$$

where the plus and minus signs hold for $k = 1$ and $k = 2$, respectively. For small z, one has the following asymptotic forms:

$$\begin{aligned} J_p(z) &\sim \frac{1}{\Gamma(p+1)}\Big(\frac{z}{2}\Big)^p \{1 + O(z^2)\}, \\ N_p(z) &\sim -\frac{\Gamma(p)}{\pi}\Big(\frac{z}{2}\Big)^{-p} \{1 + O(z^2)\} + O(z^p). \end{aligned} \tag{C.3}$$

The Hankel functions obey the identity

$$H_p^{(1)}(z)\frac{d}{dz}H_p^{(2)}(z) - H_p^{(2)}(z)\frac{d}{dz}H_p^{(1)}(z) = -\frac{4i}{\pi z}. \tag{C.4}$$

Closed form expressions exist whenever p is a half-odd-integer. We are particularly interested in the case p=3/2, which corresponds to $\mu^2 = 0$:

$$\begin{aligned} H_{3/2}^{(1)}(z) &= -\sqrt{\frac{2}{\pi z}}\, e^{iz}\Big[\frac{z+i}{z}\Big], \\ H_{3/2}^{(2)}(z) &= -\sqrt{\frac{2}{\pi z}}\, e^{-iz}\Big[\frac{z-i}{z}\Big]. \end{aligned} \tag{C.5}$$

Appendix D. Asymptotic Behavior of $\hat{\phi}_\ell^{RMS}$

In this appendix we sketch the derivations of Eqs. (6.8), (6.9), and (6.10), which describe the asymptotic behavior of $\hat{\phi}_\ell^{RMS} \equiv <\hat{\phi}_\ell^2>^{1/2}$ for very early or very late times.

In either case, one begins with the expression given by Eq. (5.3), which is valid for all times. Eq. (3.21) indicates that $z \propto e^{-\chi t}$, so at very early times the integral in Eq. (5.3) will be dominated by large values of z. Using Eq. (C.2) to describe the asymptotic behavior of the Bessel functions for large z, one has

$$<\hat{\phi}_\ell^2(t)> \sim \frac{e^{-2\chi t}}{4\pi^2}\int_0^\infty \frac{k^2\,dk\,e^{-k^2\ell^2}}{\sqrt{k^2+\gamma^2}} \times \coth\left(\frac{\sqrt{k^2+\gamma^2}}{2T_0}\right)\left\{1+O\left(\frac{\chi}{\sqrt{k^2+\gamma^2}}e^{\chi t}\right)\right\}. \tag{D.1}$$

The result (6.8) is obtained by the substitution $y \equiv 2k/T_0$.

For very late times, the integral in (5.3) is dominated by very small values of z. One then uses the asymptotic formulas (C.3) to obtain

$$<\hat{\phi}_\ell^2(t)> \sim \frac{2^{2p}\Gamma^2(p)\chi^{2p-1}}{8\pi^3}e^{(2p-3)\chi t} \times \int_0^\infty \frac{k^2\,dk\,e^{-k^2\ell^2}}{(k^2+\gamma^2)^p}\coth\left(\frac{\sqrt{k^2+\gamma^2}}{2T_0}\right)\left\{1+O\left(\frac{k^2+\gamma^2}{\chi^2}e^{-2\chi t}\right)\right\}. \tag{D.2}$$

Eq. (6.9) then follows from the substitution $y \equiv k/\gamma$.

Since the integral in (6.9b) receives its dominant contributions from y of order unity, it follows that the dominant values of k are of order $\gamma = \frac{1}{2}\sqrt{\lambda}T_0$. The dominant wavelengths are therefore longer than the mean thermal wavelength by a factor of $1/\sqrt{\lambda}$, which in our model is roughly 10^6.

To find the behavior of (6.9b) for very small λ, one uses the asymptotic approximations

$$e^{-\lambda(T_0\ell y)^2/4} \sim 1$$
$$\coth\left(\frac{1}{4}\sqrt{\lambda(y^2+1)}\right) \sim \frac{4}{\sqrt{\lambda(y^2+1)}} \tag{D.3}$$

to obtain

$$\tilde{F}^2(\lambda,\eta,T_0\ell) \sim \frac{\Gamma^2(p)}{\pi^3}\left(\frac{4}{\sqrt{\lambda}}\right)^{2p-2}\int_0^\infty \frac{y^2\,dy}{(y^2+1)^{p+\frac{1}{2}}}. \tag{D.4}$$

The result (6.10) is obtained by carrying out the integration, using the general relation[42]

$$\int_0^\infty x^{\mu-1}(1+x^2)^{\nu-1}dx = \frac{1}{2}B\left(\frac{\mu}{2},1-\nu-\frac{\mu}{2}\right) = \frac{\Gamma\left(\frac{\mu}{2}\right)\Gamma\left(1-\nu-\frac{\mu}{2}\right)}{2\Gamma(1-\nu)} \tag{D.5}$$

$$[Re\,\mu > 0, Re\left(\nu+\frac{1}{2}\mu\right) < 1].$$

REFERENCES

1. A. H. Guth, Phys. Rev. D23, 347 (1981).

2. A. D. Linde, Phys. Lett. 108B, 389 (1982).

3. A. Albrecht and P. J. Steinhardt, Phys. Rev. Lett. 48, 1220 (1982).

4. For a review, see A. D. Linde, Rep. Prog. Phys. 47, 925 (1984). For a brief summary, see A. H. Guth, in **Eleventh Texas Symposium on Relativistic Astrophysics**, ed: D. S. Evans, Ann. N. Y. Acad. Sci. 422, 1 (1984); A. H. Guth, *The New Inflationary Universe, 1984*, MIT preprint CTP# 1187, to be published in the Proceedings of the Inner Space / Outer Space Workshop (Fermilab, May, 1984); P. J. Steinhardt, Comments on Nucl. and Part. Phys. 12, 273 (1984); or S.-Y. Pi, *Progress in the Inflationary Universe*, to be published in Comments on Nucl. and Part. Phys., vol 14, no. 5 (1985).

5. A. A. Starobinsky, Phys. Lett. 117B, 175 (1982); A. H. Guth and S.-Y. Pi, Phys. Rev. Lett. 49, 1110 (1982); S. W. Hawking, Phys. Lett. 115B, 295 (1982); J. M. Bardeen, P. J. Steinhardt, and M. S. Turner, Phys. Rev. D28, 679 (1983); R. Brandenberger, R. Kahn, W. H. Press, Phys. Rev. D28, 1809 (1983); R. Brandenberger, R. Kahn, Phys. Rev. D29, 2172 (1984).

6. A. H. Guth and E. J. Weinberg, Nucl. Phys. B212, 321 (1983). S. W. Hawking, I. G. Moss, and J. M. Stewart, Phys. Rev. D26, 2681 (1982).

7. In the early models, the scalar field which drives the inflation was taken to be the same Higgs field which spontaneously breaks the grand unified gauge symmetry. However, it has been found (Ref. [5]) that in order for the mass density fluctuations to be small enough, the scalar field which drives inflation must have an extraordinarily flat potential energy function. For this reason, most of the currently acceptable models (Ref. [44]) introduce a new weakly coupled gauge-singlet scalar field for the purpose of driving the inflation. Ovrut and Steinhardt (Ref. [45]) have proposed a model in which this field also serves the purpose of breaking supersymmetry, and Pi (Ref. [46]) has suggested that inflation could be driven by the complex gauge-singlet field which gives rise to the axion.

8. A preliminary version of this material appeared as A. H. Guth and S.-Y. Pi, *The Behavior of the Higgs Field in the New Inflationary Universe*, MIT preprint CTP# 1181, to be published in the Proceedings of the Inner Space / Outer Space Workshop (Fermilab, May, 1984); also S.-Y. Pi, *Inflation-Driving Scalar Field*, Boston University preprint, Talk given at "Phase Transitions in the Early Universe" Workshop (Bielefeld, Germany, June 1984), to be published in Nucl. Phys. B.

9. The false vacuum value of ϕ is equal to zero in most models, but any other value would do just as well.

10. The properties of a de Sitter space are well described in S. W. Hawking and G.F.R. Ellis, **The Large Scale Structure of Space-Time**, Cambridge University Press (Cambridge, England, 1973).

11. G. F. Mazenko, W. G. Unruh, and R. M. Wald, Phys. Rev. D31, 273 (1985).

12. S. Coleman and E. J. Weinberg, Phys. Rev. D7, 1888 (1973).

13. S. W. Hawking and I. G. Moss, Nucl. Phys. B224, 180 (1983).

14. I. G. Moss, Phys. Lett. 128 B, 385 (1983); Nucl. Phys. B238, 436 (1984); S. W. Hawking, private communication.

15. A. D. Linde, Phys. Lett. 116B, 335 (1982).

16. A. Vilenkin and L. H. Ford, Phys. Rev. D26, 1231 (1982); A. Vilenkin, Nucl. Phys. B226, 504 (1983).

17. See, for example, G. Börner and E. Seiler, *Some Remarks Concerning the Inflationary Universe*, Max-Planck-Institut preprint, (1983); C. M. Bender and F. Cooper, Nucl. Phys. B224, 403 (1983).

18. R. H. Brandenberger, *Quantum Fluctuations as the Source of Classical Gravitational Perturbations in Inflationary Universe*, Santa Barbara ITP preprint NSF-ITP-84-03 (1984). See also the articles by Brandenberger to be published in Proc. of 8th Johns Hopkins Workshop on Current Problems in Particle Theory (Baltimore, MD, Jun 20-22, 1984), and also to be published in Proc. of the Inner Space / Outer Space Workshop (Fermilab, May 2-5, 1984).

19. J. M. Bardeen, private communication.

20. W. Bardeen and C. Hill, private communication.

21. A. Albrecht and R. Brandenberger, *On the Realization of New Inflation*, Santa Barbara ITP preprint NSF-ITP-84-145 (1984).

22. G. Semenoff and N. Weiss, Phys. Rev. D31, 689 (1985); Phys. Rev. D31, 699 (1985).

23. M. Evans and J.G. McCarthy, *On the Quantum Mechanics of Inflation*, Rockefeller University preprint RU84/B/100 (1984).

24. T. Banks, W. Fischler, and L. Susskind, *Quantum Cosmology in (2+1)-Dimensions and (3+1)-Dimensions*, SLAC preprint SLAC-PUB-3367 (1984) (Submitted to Nucl. Phys. B).

25. W. Fischler, B. Ratra, and L. Susskind, *Quantum Mechanics of Inflation*, Stanford preprint ITP-775 (1985) (Expanded version).

26. A rather thorough discussion of the upside-down harmonic oscillator is given by G. Barton, *Quantum Mechanics of the Inverted Oscillator Potential*, to be published in Ann. Phys. (N.Y.). He does not, however, discuss the classical nature of the solution

at large times.

27. When we say that a function $f(x,t)$ is $O(g(t))$, we mean that $|f(x,t)/g(t)|$ is bounded for each x as $t \to \infty$.

28. S. Weinberg, Phys. Rev. D9, 3357 (1974).

29. D. A. Kirzhnits and A. D. Linde, Phys. Lett. 42B, 471 (1972); L. Dolan and R. Jackiw, Phys. Rev. D9, 3320 (1974); for a review, see A. D. Linde, Rep. Prog. Phys. 42, 389 (1979).

30. For the benefit of newcomers to de Sitter space, we point out that the expansion of this space provides an event horizon. If two observers that are comoving in the coordinate system described by (3.1) are separated at a given time by a physical distance χ^{-1} (i.e., a coordinate distance $\chi^{-1}e^{-\chi t}$), then a light pulse emitted by one observer at the given time will never reach the other observer.

31. G. W. Gibbons and S. W. Hawking, Phys. Rev. D15, 2738 (1977).

32. T. S. Bunch and P. C. W. Davies, Proc. Roy. Soc. London, Ser. A 360, 117 (1978).

33. The rate of thermalization for standard gauge theories is calculated by J. Ellis and G. Steigman, Phys. Lett. 89B, 186 (1980). The much weaker coupling for our case will mean that thermalization does not have time to occur.

34. L. D. Landau and E. M. Lifshitz, **Statistical Physics**, Addison-Wesley (Reading, Massachusetts, 1969), pp. 83-86.

35. We thank Jim Peebles for calling our attention to this fact.

36. A. H. Guth and S.-Y. Pi, Ref. [5].

37. It is demonstrated in a footnote in Ref. [36] that this limit exists for arbitrary $V(\phi)$. The key point is that for large times $\delta\phi(\vec{x},t)$ and $\dot{\phi}_0(t)$ obey the same second order differential equation. One of the two linearly independent solutions dominates at large times, so both $\delta\phi$ and $\dot{\phi}_0$ share the same large time asymptotic behavior.

38. Note that Eq. (3.6) of Ref. [32] is misprinted, and should read $\psi_k(\eta) = \alpha^{-1}(\pi/4)^{1/2} \times \eta^{3/2} H_\nu^{(2)}(k\eta)$.

39. This matching condition, used in Ref. [36], is roughly equivalent to the frequently used rule of thumb that $\delta\phi$ is of order χ when the wavelength equals the Hubble length.

40. Note that our expression differs from that of Ref. [32] in two compensating ways: the Hankel functions $H_p^{(1)}(z)$ and $H_p^{(2)}(z)$ are reversed, and so is the sign of z. We have chosen our conventions to avoid using the Hankel functions on the negative real axis, where they are usually defined to have a branch cut.

41. Note that the wave function (B.7) can also be obtained quite easily by the operator methods of Section III. Using Eq. (3.30) for the annihilation operator a_α and (3.22) for $\pi_\alpha \equiv -i\hbar\partial/\partial\sigma_\alpha$, one can find $\Psi_\alpha(\sigma_\alpha,t)$ by solving the equation $a_\alpha|\Psi_\alpha> = 0$.

42. I. S. Gradshteyn and I. M. Ryzhik, **Tables of Integrals, Series, and Products**, Academic Press (New York, 1965).

43. M. Abramowitz and I. A. Stegun, **Handbook of Mathematical Functions with Formulas, Graphs, and Mathematical Methods**, Dover Press (New York, 1972).

44. J. Ellis, D. V. Nanopoulos, K. A. Olive, and K. Tamvakis, Nucl. Phys. B221, 524 (1983); D. V. Nanopoulos, K. A. Olive, M. Srednicki, and K. Tamvakis, Phys. Lett. 123B, 41 (1983); D. V. Nanopoulos, K. A. Olive, and M. Srednicki, Phys. Lett. 127B, 30 (1983); G. B. Gelmini, D. V. Nanopoulos, and K. A. Olive, Phys. Lett. 131B, 53 (1983); D. V. Nanopoulos and M. Srednicki, Phys. Lett. 133B, 287 (1983); B. A. Ovrut and P. J. Steinhardt, Phys. Lett. 133B, 161 (1983), Phys. Rev. Lett. 53, 732 (1984), and Phys. Lett. 147B, 263 (1984); B. A. Ovrut and S. Raby, Phys. Lett. 134B, 51 (1984); Q. Shafi and A. Vilenkin, Phys. Rev. Lett. 52, 691 (1984); P. Q. Hung, Phys. Rev. D30, 1637 (1984); S. Gupta and H. R. Quinn, Phys. Rev. D29, 2791 (1984); R. Holman, P. Ramond, and G. G. Ross, Phys. Lett. 137B, 343 (1984); S.-Y. Pi, Phys. Rev. Lett. 52, 1725 (1984); Q. Shafi and F. W. Stecker, Phys. Rev. Lett. 53, 1292 (1984).

45. B. A. Ovrut and P. J. Steinhardt, Ref. [44].

46. S.-Y. Pi, Ref. [44].

FIGURE CAPTIONS

Figure 1: The generic behavior of the finite-temperature effective potential for the scalar field in the new inflationary universe model.

Figure 2: At late times the particle moves along a classical trajectory $x(t) = \pm be^{\omega(t-\tau)}$, where τ is a random variable with a probability density $P(\tau)$ shown in the graph above.

Figure 3: Graph (a) shows the potential energy function $V(x)$ for a one-dimensional quantum mechanical tunneling problem, and graph (b) shows the form of the probability density $|\psi|^2$ for the steady-state solution. As in the case of the upside-down harmonic oscillator, the wave function at large x describes a state which is accurately approximated by a probability distribution of classical trajectories.

Figure 4: A plot of the potential energy function $V(\phi)$ given in Eq. (3.4).

Figure 5: The root-mean-square value of the Fourier coefficients $\sigma_\alpha(t)$ are given by the square root of the right-hand side of Eq. (3.34). The time-dependence arises from the first non-trivial factor, $|\psi(\vec{k}_\alpha, t)|$, and is shown in plot (a) for several values of $\eta \equiv \mu^2/\chi^2$. The midpoint of the graph corresponds to the time when $z = 1$, which means that the "effective wave number" $e^{-\chi t}\sqrt{\vec{k}_\alpha^{\,2} + \gamma^2}$ is equal to χ, the inverse of the de Sitter horizon distance. The second factor, $\sqrt{\coth(\frac{1}{2}\Theta_\alpha)}$, represents the enhancement due to thermal effects. It is shown in plot (b) as a function of the effective temperature $\Theta_\alpha^{-1} = T_0/(H\sqrt{\vec{k}_\alpha^{\,2} + \gamma^2})$.

Figure 6: The variation of $\hat{\phi}_\ell^{RMS} \equiv [< \hat{\phi}_\ell^2 >]^{1/2}$ with t, shown for $\eta = 0.2$ and $\lambda = 10^{-12}$. The zero of time has been fixed by setting $T_0 \equiv \chi$, which means that $T = \chi$ when $t = 0$. The smearing length has been chosen as $\ell = T_0^{-1}$. The point where $\phi = \phi_c$ is labelled A, the point where $T = T_c$ is labelled B, the point where $T = T_{deS}$ (i.e., when the thermal and false vacuum energy densities are about equal) is labelled C, and the point where $T = \chi$ is labelled D.

Figure 7: The behavior of $\hat{\phi}_\ell^{RMS}$ for various values of η. All the curves are drawn for $T_0 \equiv \chi$, $T_0\ell = 1$, and $\lambda = 10^{-12}$. On each curve, A denotes the point at which $\hat{\phi}_\ell^{RMS} = \phi_c$, B denotes $T = T_c$, C denotes $T = T_{deS}$, and D denotes $T = \chi$.

Figure 8: The behavior of $\hat{\phi}_\ell^{RMS}$ for various values of $T_0\ell$. All the curves are drawn for $\eta = 0.2$, $T_0 \equiv \chi$, and $\lambda = 10^{-12}$. The upper three curves are drawn for fixed values of $T_0\ell$, corresponding to smearing over a fixed coordinate wavelength. The lower three curves correspond to fixed values of $T_0\ell e^{\chi t}$, so in this case the physical smearing length is held fixed.

Figure 9: The behavior of $\hat{\phi}_\ell^{RMS}$ for various values of λ. All the curves are drawn for $\eta = 0.2$ and $T_0 \equiv \chi$. The upper curves show the effect of a fixed coordinate smearing length ($T_0\ell = 1$) and the lower curves show a fixed physical smearing length ($T_0\ell e^{\chi t} = 1$).

Figure 10: The maximum acceptable value of λ as a function of $\eta \equiv \mu^2/\chi^2$. If λ exceeds this value, then it is unlikely that an arbitrary region will undergo sufficient inflation to explain the large scale homogeneity of the observed universe.

Figure 11: The ratio of the exact computation of $\Delta\rho/\rho$ to an approximate calculation of the same quantity is shown as a function of $\eta \equiv \mu^2/\chi^2$.

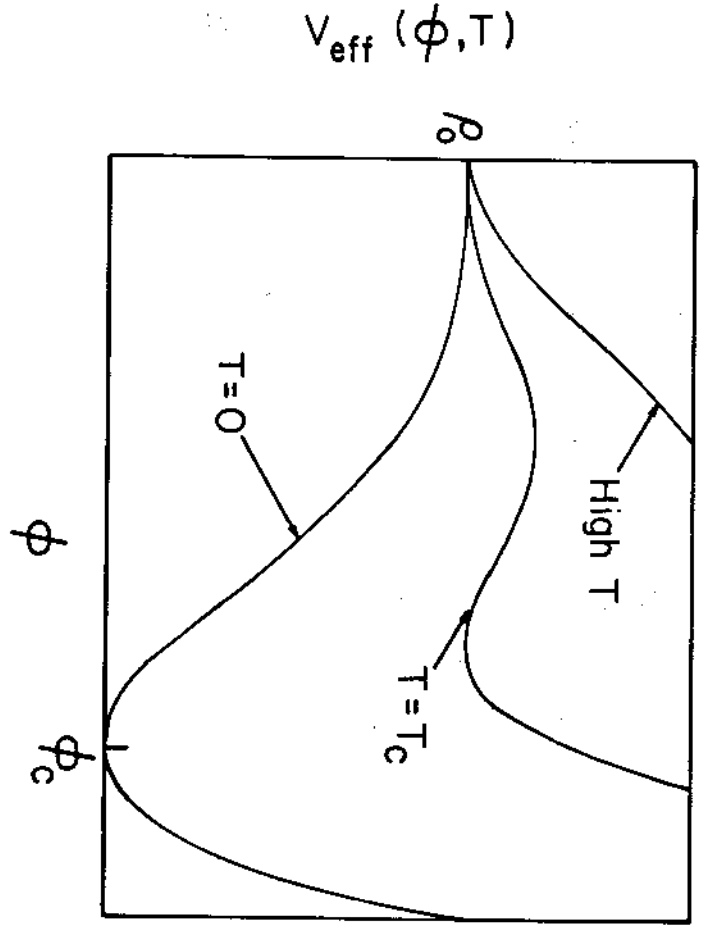

FIGURE 1

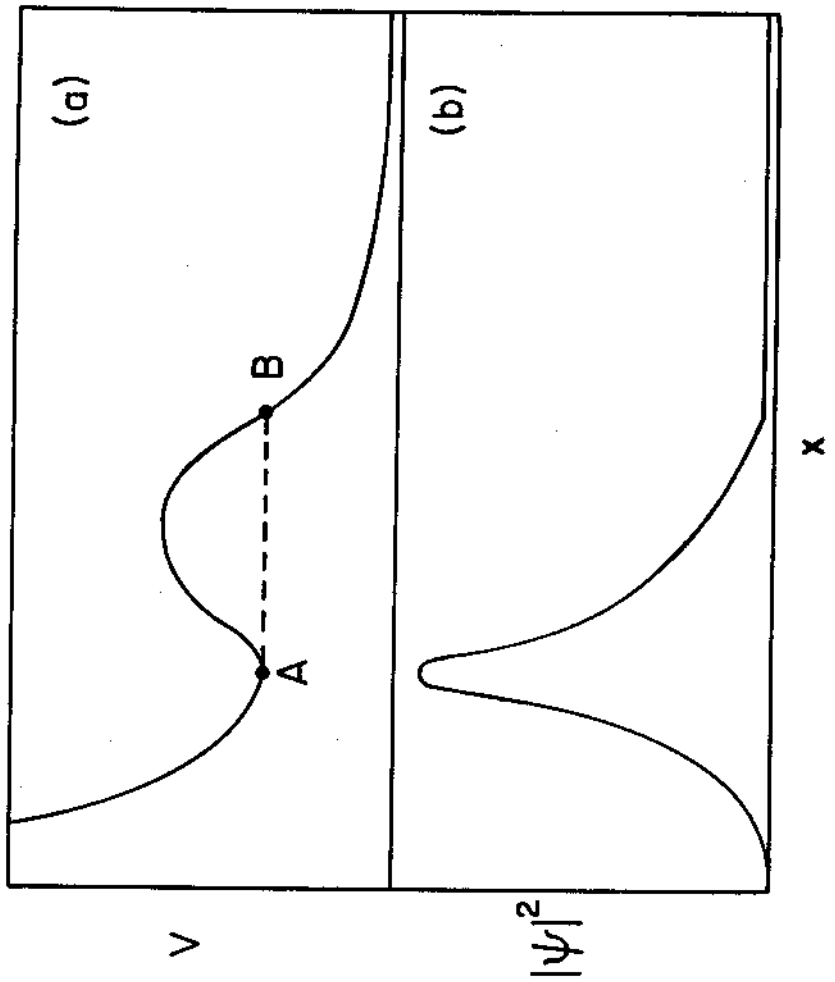

FIGURE 3

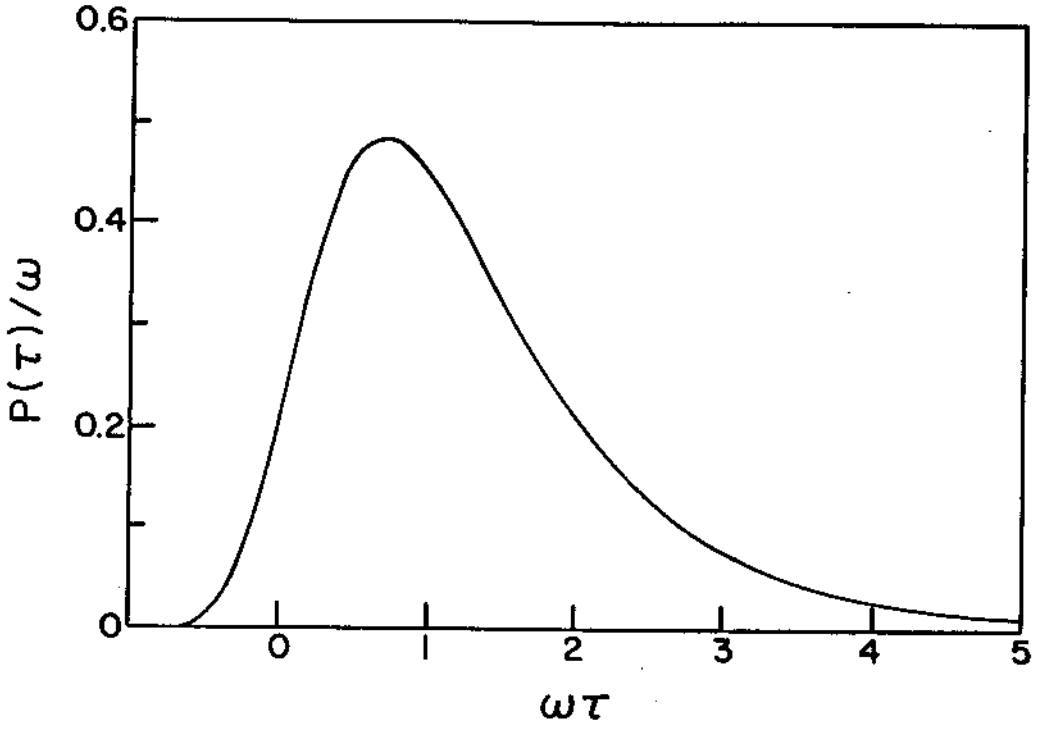

FIGURE 2

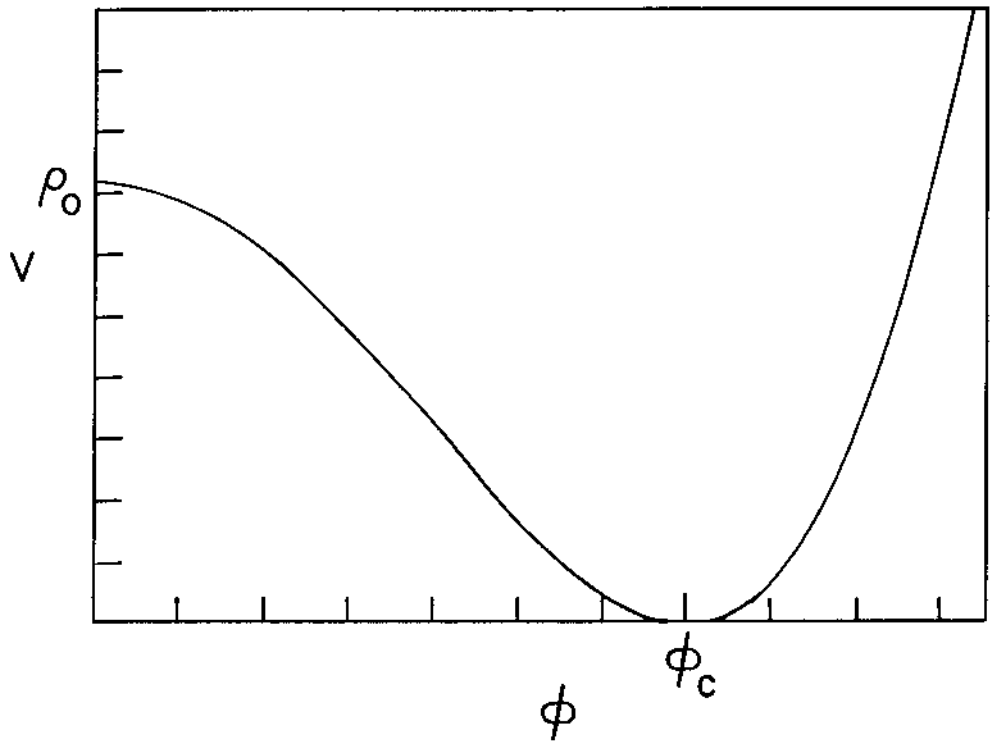

FIGURE 4

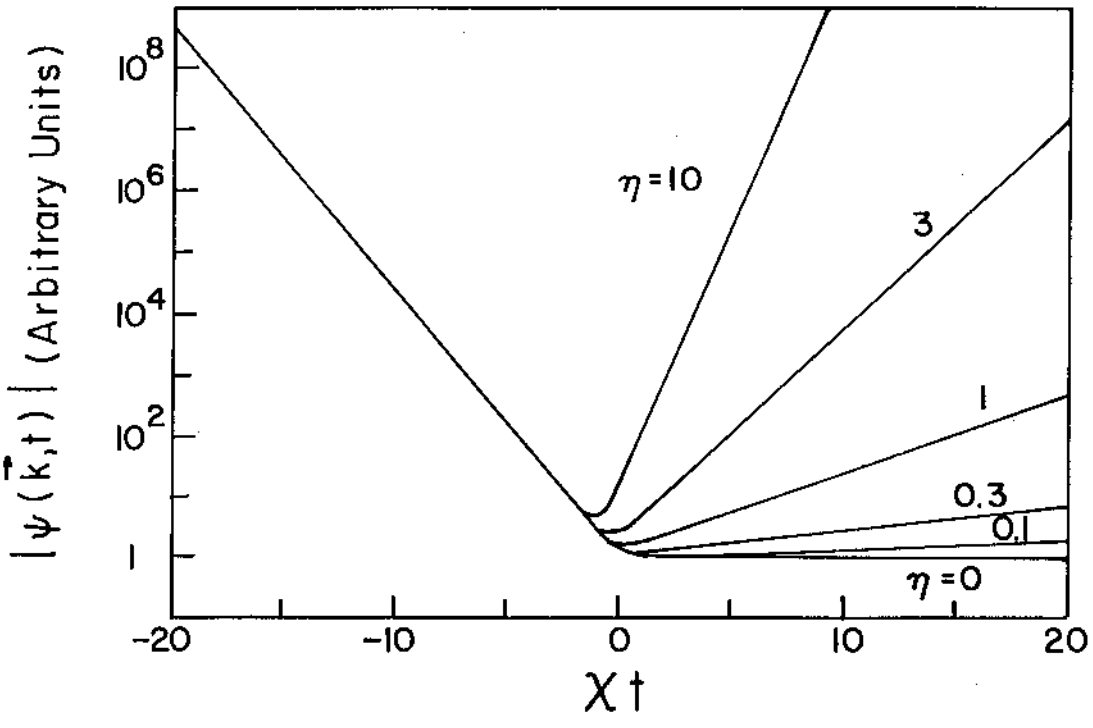

FIGURE 5A

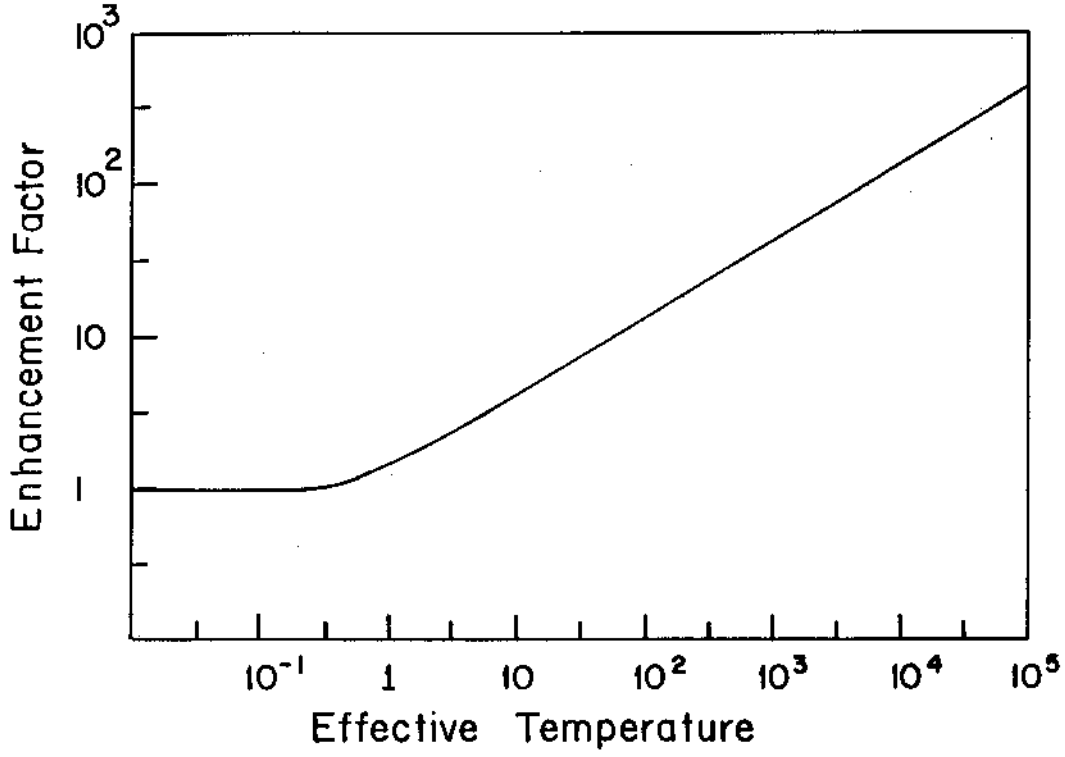

FIGURE 5B

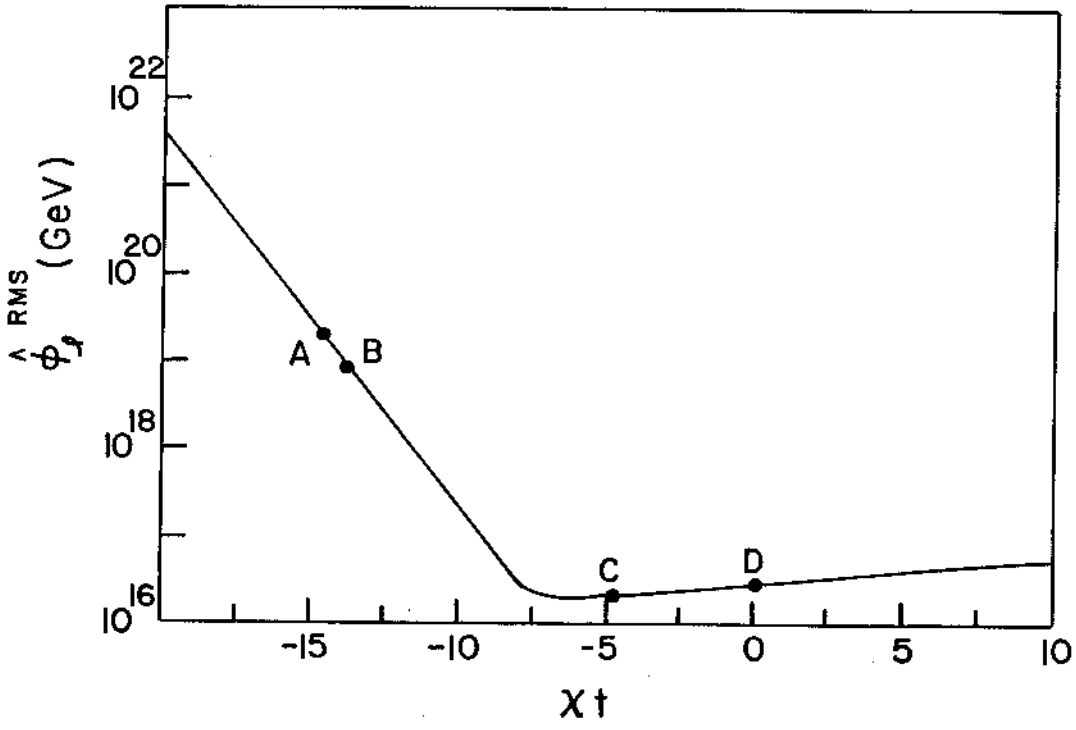

FIGURE 6

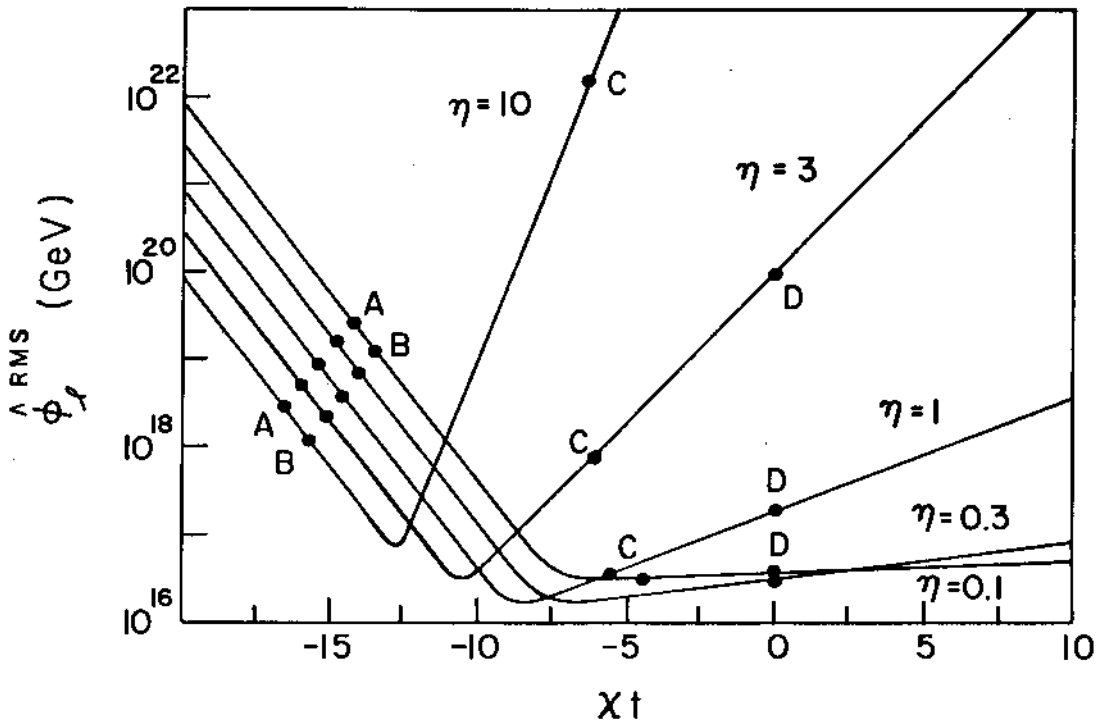

FIGURE 7

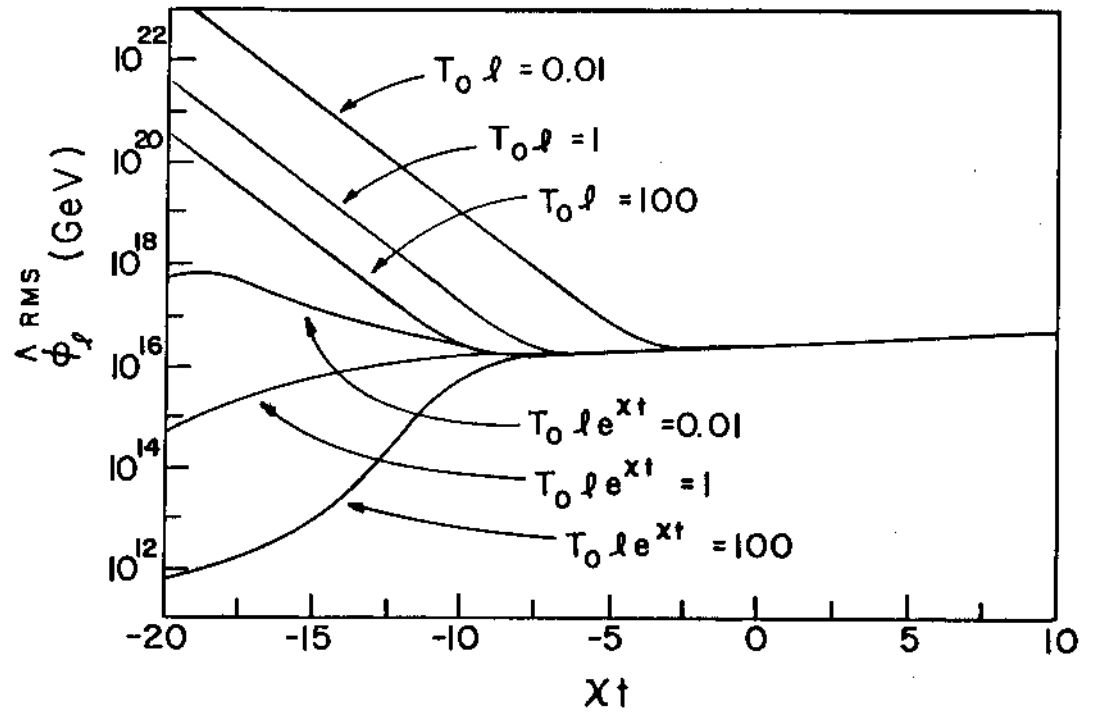

FIGURE 8

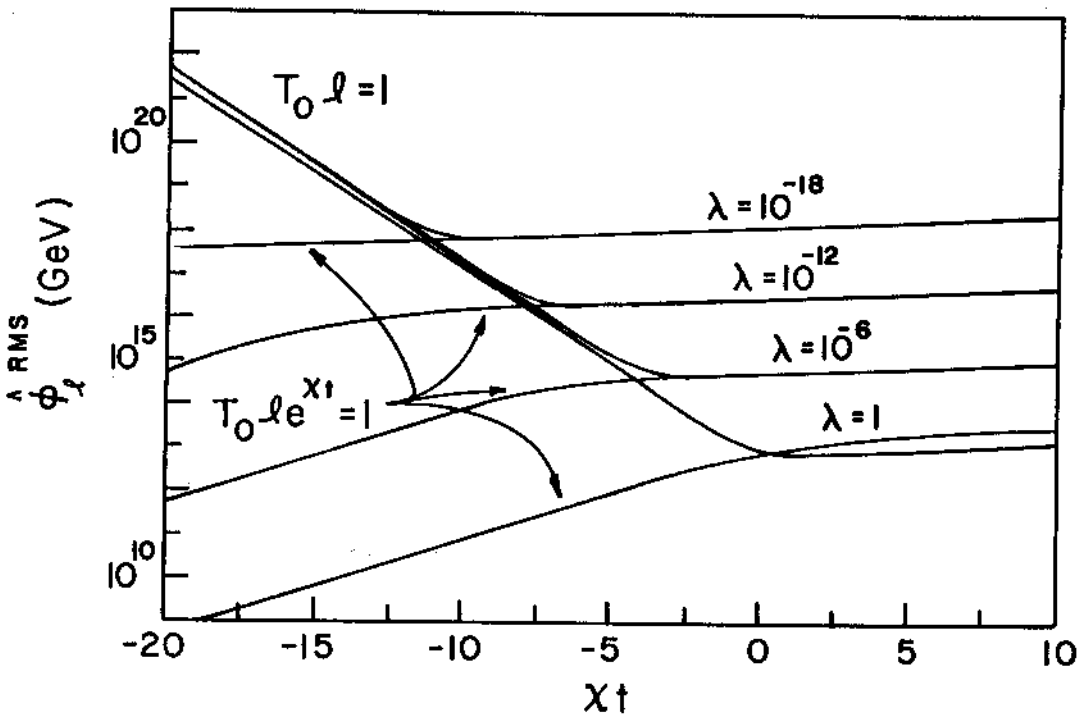
$T_0 \ell = 1$
$\lambda = 10^{-18}$
$\lambda = 10^{-12}$
$\lambda = 10^{-6}$
$\lambda = 1$
$T_0 \ell e^{\chi t} = 1$
$\hat{\phi}^{RMS}_{\ell}$ (GeV)
10^{20}
10^{15}
10^{10}
-20
-15
-10
-5
0
5
10
χt

FIGURE 9

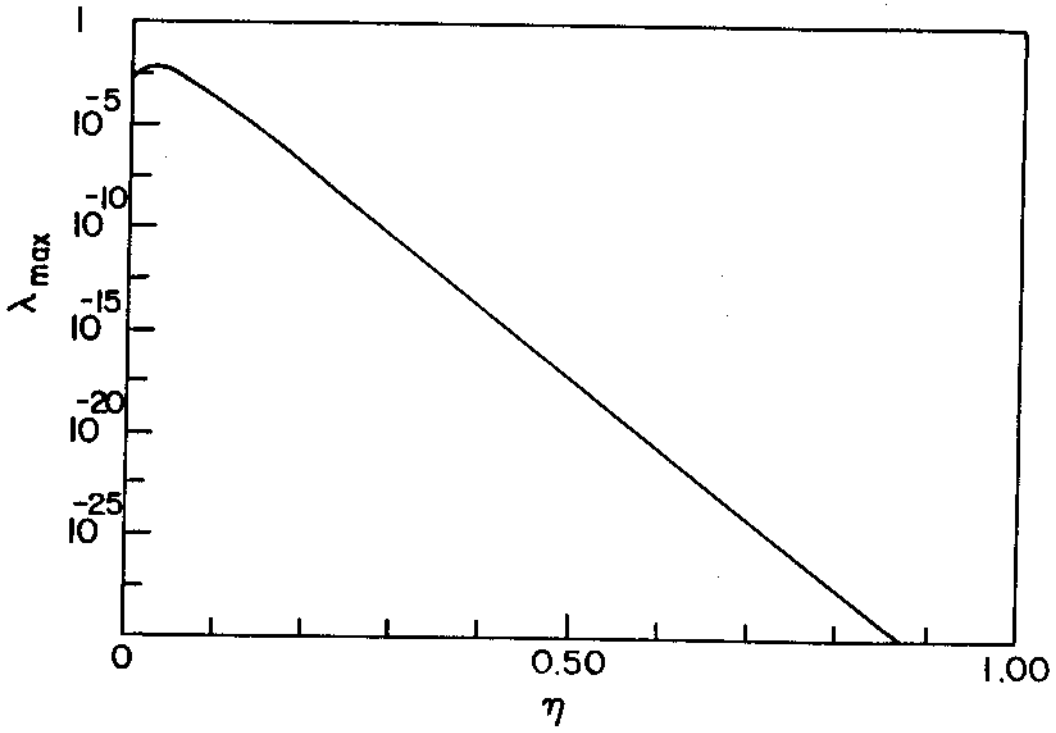
1
10^{-5}
10^{-10}
10^{-15}
10^{-20}
10^{-25}
λ_{max}
0
0.50
1.00
η

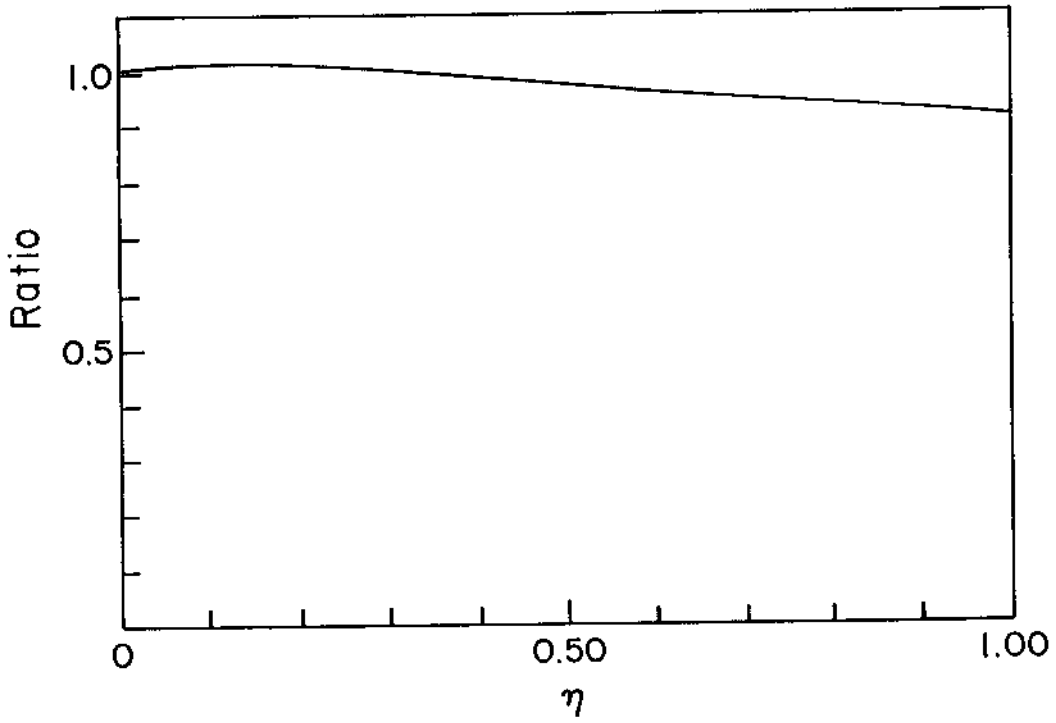

FIGURE 11